CDK1-induced regulation of p53 phosphorylation at Ser315 mediates cell cycle arrest and apoptosis of macrophages infected with clinical isolates of *Mycobacterium tuberculosis*

BANGHAO SUN[1,2*], ZHENYU ZHAO[3*], QINGYU MENG[2,4], LUYA PU[2,5], XINGYU JIANG[2], SHUAI LI[2], FADI CAO[2] and FAN LI[1,2]

[1]Department of Immunology, School of Basic Medical Sciences, Xinjiang Medical University, Urumqi, Xinjiang 830000, P.R. China; [2]Department of Pathogen Biology, The Key Laboratory of Zoonosis, Chinese Ministry of Education, College of Basic Medicine, Jilin University, Changchun, Jilin 130021, P.R. China; [3]School and Hospital of Stomatology, Jilin University, Changchun, Jilin 130021, P.R. China; [4]Department of Laboratory, China-Japan Union Hospital of Jilin University, Changchun, Jilin 130021, P.R. China; [5]Vascular Surgery Department, China-Japan Union Hospital of Jilin University, Changchun, Jilin 130021, P.R. China

Received April 10, 2025; Accepted October 10, 2025

DOI: 10.3892/mmr.2025.13754

Abstract. Tuberculosis (TB) is an infectious disease caused by infection with *Mycobacterium tuberculosis* (MTB). The morbidity of TB in the Xinjiang region of China is higher than that in other provinces. Macrophage apoptosis after infection with MTB is considered to serve a key role in killing the bacteria. However, the biological process of apoptosis and the underlying molecular mechanisms triggered by the infection of macrophages with clinical isolates of MTB from Xinjiang (XJMTB) are not clear. The present study aimed to investigate the unique characteristics of XJMTB. Briefly, western blotting and flow cytometry were employed in the present study, and it was demonstrated that macrophages infected with MTB H37Rv or XJMTB underwent G_2/M cell cycle arrest and apoptosis. The transcriptome sequencing analysis showed that cyclin-dependent kinase 1 (CDK1) was a key regulatory gene in regulating the G_2/M cell cycle arrest and apoptosis in MTB-infected macrophages, and the p53 gene was most likely involved in the regulation of this. Moreover, the phosphorylation of p53 (Ser315) was elevated with the upregulation of CDK1 activation, leading to a higher proportion of MTB-infected macrophages exhibiting G_2/M cell cycle block and apoptosis. The current study also revealed that enhanced activation of CDK1 reversed the attenuation of the G_2/M cell cycle block and the reduction in the percentage of apoptosis caused by inhibition of p53 (Ser315) phosphorylation. Furthermore, the co-immunoprecipitation experiment demonstrated an interaction between CDK1 and p53. The present study indicated that, in an *in vitro* model of macrophage infection with XJMTB, enhanced activation of CDK1 may regulate the phosphorylation of p53 (Ser315), promote the secretion of TNF-α, IL-6, IL-10, IL-1β and IL-12, promote G_2/M cell cycle arrest and apoptosis of macrophages, and enhance the survival of XJMTB in macrophages. These results provide CDK1 and phosphorylated-p53 as two new potential therapeutic targets for TB in Xinjiang, and lay a foundation for the development of novel TB treatment strategies.

Introduction

Tuberculosis (TB) is an infectious disease caused by *Mycobacterium tuberculosis* (MTB) infection. Globally, there are ~10 million new cases of TB and 1.6 million TB-related deaths annually, making it the leading source of infection and one of the top ten causes of death. Notably, China is one of 30 countries with a high morbidity rate of TB (1). The Chinese Center for Disease Control and Prevention has shown that the geographical distribution of TB epidemics in China is characterized by low incidence in the eastern region and high prevalence in the western region, and the incidence rate of TB is higher in the Xinjiang region than in other provinces (2,3). The average rate of culture-positive TB is 119/100,000 people in China, whereas it is 433/100,000 in the Xinjiang region (4). The high prevalence rate of TB in Xinjiang may be due to unique climatic, geographic and demographic characteristics (5), as well as the high incidence of HIV infection, the growing floating population, unhealthy habits and poor living conditions in rural areas; however, the exact reason is unclear.

MTB is an intracellular pathogen and macrophages are major innate immune cells, which are the first line of defense against MTB infection and the primary effector cells for clearing this pathogen (6,7). To avoid becoming reservoirs of

Correspondence to: Professor Fan Li, Department of Immunology, School of Basic Medical Sciences, Xinjiang Medical University, 393 Xinyi Street, Urumqi, Xinjiang 830000, P.R. China
E-mail: lifan@jlu.edu.cn

*Contributed equally

Key words: tuberculosis, CDK1, phosphorylated-p53, cell cycle, apoptosis

MTB, host macrophages have evolved a number of defense mechanisms, including autophagy (8) and apoptosis (9), to kill or prevent the growth of MTB. Immune cell apoptosis is an important mechanism against bacterial and viral infections, and some studies have suggested that macrophage apoptosis induced by MTB infection can kill MTB (10,11). However, other studies have suggested that excessive apoptosis is conducive to MTB survival (12,13). Thus, a clear understanding of the interaction of MTB with host macrophages may help develop targeted strategies for controlling TB.

Cyclin-dependent kinase 1 (CDK1) is a member of the CDK protein family, and it controls all aspects of cell division, including cell cycle entry from quiescence, G_1/S phase transition, DNA replication in the S phase, nuclear rupture, chromosome cohesion and segregation, and cytoplasmic division (14-16). CDK1 is a proline-directed kinase that phosphorylates a large number of proteins to drive cell cycle progression and specific processes associated with different cell cycle phases (15). Huang *et al* (17) showed that CDK1 can regulate the degree of cell cycle arrest during the G_2/M phase. Furthermore, previous studies have shown a close association between CDK1 and tumor cell apoptosis in glioblastoma (18), human hepatocellular carcinoma (19), cervical carcinoma (20), colorectal carcinoma (21,22) and ovarian carcinoma (23). However, the role of CDK1 in the immune response of macrophages after TB infection is unclear.

The transcription factor p53, once activated by phosphorylation and acetylation, binds directly to specific DNA sequences in the promoter region of target genes to regulate their expression (24,25). Notably, p53 target genes are involved in the regulation of apoptosis, DNA repair, cell cycle arrest, senescence and programmed cell death (25-27). It has been shown that promoting phosphorylation of the p53 protein can enhance macrophage apoptosis and suppress the survival of MTB-infected macrophages (28).

The present study utilized bioinformatics analysis to investigate the effects of the CDK1 gene on the apoptosis and cell cycle progression of macrophages infected with different sources of MTB *in vitro*. The current study aimed to reveal the specific immune response involving CDK1 and phosphorylated (p)-p53 in macrophages after infection with MTB clinical isolates, as well as the mechanism by which CDK1 and p-p53 regulate macrophage cycle arrest and apoptosis after infection with MTB from Xinjiang (XJMTB). CDK1 and p-p53 may be considered novel treatment targets for TB in Xinjiang and lay the foundation for formulating TB treatment strategies.

Materials and methods

Sample collection, and MTB resuscitation, isolation and culture. The sputum samples of 20 cases were derived from 103 patients with sputum smear-positive TB in the Xinjiang region during a previous epidemiological survey conducted by the cooperative team (29). All cases were diagnosed according to China's national diagnostic criteria (30). Demographic, epidemiological and clinical data were obtained from the medical records of the patients using a unified epidemiological survey methodology. Table I provides the details of the 20 patients.

The sputum was mixed with 1-3 times the volume of a 4% NaOH (Beijing Chemical Works) solution, shaken well until dissolved and maintained at room temperature for 20 min. Once the sample was completely liquefied, 100 μl sample was aspirated and dropped evenly on the slant of modified acidic Roche's medium (Celnovte Biotechnology Co., Ltd.). Each sample was inoculated three times and placed in a 37˚C incubator. After a single white colony was grown, it was picked off, placed in a 37˚C incubator containing 40 ml *Mycobacterium* liquid medium (Shanghai Jingnuo Biotechnology Co., Ltd.) and shaken at 120 rpm for amplification. In addition, 50-100 μl frozen H37Rv (cat. no. 27294; American Type Culture Collection) bacterial solution was aspirated, added to 40 ml *Mycobacterium* liquid medium and amplified by shaking at 120 rpm.

Acid-fast staining. An inoculation loop was dipped into the XJMTB amplified bacterial solution, applied onto a slide and fixed by heating alone. Subsequently, carbol fuchsin was added dropwise to the solution, the solution was slowly heated (but not boiled) for 3-5 min and washed with water. Hydrochloric acid-ethanol solution (3%) was then added dropwise to the solution to decolorize it for 30 sec. Finally, methylene blue was added dropwise to the solution for 0.5-1 min, after which the slide was washed, dried and observed under an optical microscope with oil immersion.

Strain typing and identification of clinical isolates of MTB. Briefly, 100 μl amplified bacilli were dropped evenly onto para-nitrobenzoic acid (PNB) and thiophene-2-carboxylic acid hydrazide (TCH) media (Celnovte Biotechnology Co., Ltd.), with each sample inoculated three times, and cultured at 37˚C with 5% CO_2. Observations were made weekly, and the results were determined after 4 weeks. A single colony growing on the culture medium indicates a positive result, with negative PNB and positive TCH considered MTB infection.

For strain typing, the DNA of MTB was extracted using a bacterial DNA extraction kit (cat. no. R0017S; Beyotime Institute of Biotechnology), and the MIRU 26 fragment was amplified using a PCR kit with Taq (cat. no. D7232; Beyotime Institute of Biotechnology). The PCR thermocycling conditions were as follows: i) 94˚C for 3 min (1 cycle); ii) 30 cycles at 94˚C for 30 sec, 55˚C for 30 sec and 72˚C for 60 sec; iii) 72˚C for 10 min (1 cycle), iv) maintained at 4˚C. The MIRU 26 primer sequences were: Forward primer 5'-3': TAGGTCTAC CGTCGAAATCTGTGAC, reverse primer 5'-3': CATAGG CGACCAGGCGAATAG. Agarose (cat. no. ST118; Beyotime Institute of Biotechnology) and Gel-Green (cat. no. D0143; Beyotime Institute of Biotechnology) were used to prepare 1% agarose gel, and the PCR products were electrophoresed at 130 V and observed using a Tanon-1600 Gel Image system (Tianneng Science and Technology Co., Ltd.).

Cell culture and modeling of MTB infection. The THP-1 human monocyte cell line was purchased from The Cell Bank of Type Culture Collection of The Chinese Academy of Sciences. The cells were inoculated at a concentration of $1x10^6$ cells/ml in 6-well plates (1 ml cell suspension/well) in RPMI 1640 medium (Gibco; Thermo Fisher Scientific, Inc.) supplemented with 10% fetal bovine serum (Gibco; Thermo Fisher Scientific, Inc.), and serum-free RPMI 1640 medium with an equal amount of phorbol-12-myristate-13-acetate (PMA; MedChemExpress) at a concentration of 400 ng/ml

Table I. Patient's basic information.

Number	Sex	Age, years	Ethnicity	Separation and amplification	TCH	PNB
L1	Male	35	Han	Yes	+	+
L2	Male	32	Uighur	Yes	-	-
L3	Male	25	Uighur	Yes	+	-
L4	Female	52	Han	Yes	+	-
L5	Female	38	Han	Yes	+	-
L6	Male	42	Uighur	Yes	+	-
L7	Male	56	Han	Yes	+	-
L8	Female	43	Uighur	Yes	+	-
L9	Male	44	Uighur	Yes	+	-
L10	Male	47	Han	No	/	/
L11	Female	37	Uighur	No	/	/
L12	Male	55	Uighur	Yes	+	-
L13	Female	28	Uighur	No	/	/
L14	Male	37	Han	Yes	+	-
L15	Female	45	Han	No	/	/
L16	Male	29	Uighur	Yes	+	-
L17	Female	26	Han	Yes	+	-
L18	Male	53	Han	Yes	+	-
L19	Male	28	Uighur	Yes	-	-
L20	Female	57	Han	Yes	+	-

PNB, para-nitrobenzoic acid; TCH, thiophene-2-carboxylic acid hydrazide; /, PNB and TCH media were not identified due to separation failure.

was added to induce cell differentiation into macrophages for 24 h. After removing the culture medium containing PMA, an equal volume of fresh RPMI 1640 complete culture medium was added. H37Rv and XJMTB were diluted to an OD600 of 0.6 in *Mycobacterium* liquid medium, and 100 μl of the fluid was added to each well to infect cells for 12, 24 and 36 h. Finally, MTB samples isolated from the sputum samples of patients numbered L3-L6 (Beijing family) were used for L group modeling in the current study. H37Rv was used for V group modeling in the current study. THP-1 cells used for transcriptome sequencing were divided into three groups: XJMTB clinical isolate-infected group (L group), H37Rv standard strain-infected group (V group) and blank control group not infected with any bacteria (C group). All cell culture conditions were as follows: 37˚C, 5% CO_2.

Enzyme-linked immunosorbent assay (ELISA). Culture supernatants were centrifuged at 300 x g for 10 min at room temperature. Subsequently, the secretion levels of cytokines in the cell culture supernatants were measured using sandwich ELISA detection kits for IL-12p70 (cat. no. EK112), TNF-α (cat. no. EK182), IL-6 (cat. no. EK1153), IL-1β (cat. no. EK101B) and IL-10 (cat. no. EK110) [Multisciences (Lianke) Biotech, Co., Ltd.]. All operations were performed according to the manufacturer's protocol. The absorbance was measured using a microplate reader at 450 nm and compared to a standard curve.

Nitric oxide (NO) measurement assay. To evaluate NO levels during MTB infection, cell culture supernatants were analyzed using the Griess assay. Culture supernatants were centrifuged at 300 x g for 10 min at room temperature. Subsequently, the supernatant (100 μl) was incubated with Griess reagent (cat. no. G4410; Sigma-Aldrich; Merck KGaA) (100 μl) at room temperature for 10 min, and the absorbance was then measured at 541 nm. Sodium nitrite was used to create a standard concentration curve.

RNA isolation and library preparation. Total RNA was extracted from the aforementioned three groups of THP-1 cells using Trizol reagent (cat. no. R0016; Beyotime Institute of Biotechnology). The extracted RNA was quantified and assessed for purity and integrity using a NanoDrop 2000 spectrophotometer (NanoDrop; Thermo Fisher Scientific, Inc.) and an Agilent 2100 Bioanalyzer (Agilent Technologies, Inc.). Subsequently, library construction was performed using TruSeq Stranded Total RNA Library Prep Kit with Ribo-Zero Gold (cat. no. RS-122-2301; Illumina, Inc.). The amount of RNA used to construct the library was 1 μg. Ribosomal RNA (rRNA) removal was performed using the Ribo-Zero Gold rRNA Removal Kit (Illumina, Inc.). Subsequently, sequencing libraries were constructed using rRNA-depleted samples. Finally, products were purified (Agencourt AMPure XP; Beckman Coulter, Inc.), and library quality was assessed using the Agilent 2100 Bioanalyzer system.

Transcriptome sequencing and differentially expressed gene (DEG) analysis. The libraries were sequenced on the Illumina HiSeq X Ten platform (Illumina, Inc.) to produce 150 bp paired-end reads. In this step, clean data

Table II. Primer sequences used for reverse transcription-quantitative polymerase chain reaction.

Primer name	Forward primer 5'-3'	Reverse primer 5'-3'
CCNA2	AGAAACAGCCAGACATCACTAA	TTCAAACTTTGAGGCTAACAGC
CDK1	CACAAAACTACAGGTCAAGTGG	GAGAAATTTCCCGAATTGCAGT
β-actin	GGCCAACCGCGAGAAGATGAC	GGATAGCACAGCCTGGATAGCAAC

CCNA2, cyclin A2; CDK1, cyclin-dependent kinase 1.

(clean reads) were obtained by removing reads containing adapters and ploy-N (sequencing errors or insufficient sequencing quality) or low-quality reads from the raw data. Sequencing reads were mapped to the human genome (GRCh38) using HISAT2 (31). For mRNA, FPKM was calculated for each gene using Cufflinks (1.2) (32), and read counts were obtained for each gene using HTSeq-Count (0.12.3) (33). RNA expression profiling data were analyzed using the R (3.6.3) (https://www.r-project.org/) software package DESeq2 (1.26.0) (https://bioconductor.org/packages/release/bioc/html/DESeq2.html). The package pheatmap (1.0.12) (https://cran.r-project.org/package=pheatmap) in R (3.6.3) was used to create heat maps, whereas the package ggplot2 (3.3.5) (https://cran.r-project.org/web/packages/ggplot2/index.html) was used to create volcano maps. Bioinformatics & Evolutionary Genomics (http://bioinformatics.psb.ugent.be/webtools/Venn/) was used for creating Venn diagrams. Principal component analysis (PCA) was performed using the OECloud tools at https://cloud.oebiotech.com. The |log2 fold change|≥1 and P≤0.05 were used as criteria to screen significant DEGs for subsequent analysis. STRING (https://cn.string-db.org/cgi/input?sessionId=bTEPyYc5wXuA&input_page_show_search=off) was used to perform the protein-protein interaction (PPI) network analysis, and Cytoscape (3.8.1) (https://cytoscape.org/) and its MCODE plugin (34) was used to perform subnetwork screening and confirmation.

Gene ontology (GO) and kyoto encyclopedia of genes and genomes (KEGG) enrichment analyses. The Database for Annotation, Visualization, and Integrated Discovery (https://davidbioinformatics.nih.gov/) was used for functional analysis of DEGs. The significant GO biological processes and KEGG pathways with an adjusted P<0.05 were selected to analyze their biological function. The significant enrichment results were visualized using the ggplot2 (3.3.5) (https://cran.r-project.org/web/packages/ggplot2/index.html) package of R software (3.6.3).

Reverse transcription-quantitative polymerase chain reaction (RT-qPCR). Total RNA was extracted from cultured cells using TRIzol reagent. mRNA was reverse transcribed into cDNA using the HiScript II 1st Strand cDNA Synthesis Kit (Vazyme Biotech Co., Ltd.), according to manufacturer's protocol. qPCR was performed to measure mRNA using the ABI 7300 Plus Real-Time PCR System (Applied Biosystems; Thermo Fisher Scientific, Inc.) using the FastStart Universal SYBR Green Master Mix (Roche Diagnostics). The qPCR thermocycling conditions were as follows: i) 50˚C for 2 min (1 cycle); ii) 95˚C for 10 min (1 cycle); iii) 40 cycles of denaturation at 95˚C for 15 sec, and annealing and extension at 60˚C for 60 sec. β-actin was used as the endogenous control for mRNA expression and relative fold changes were calculated using the $2^{-\Delta\Delta Cq}$ method (35). Each RT-qPCR assay was repeated three times. The primer sequences used are shown in Table II.

Western blotting. Cells were lysed using RIPA buffer (MilliporeSigma) supplemented with EDTA-Free 1x Halt™ protease and phosphatase inhibitor (Thermo Fisher Scientific, Inc.). The cell lysate was then centrifuged at 14,000 x g for 15 min at 4˚C and the protein concentration was determined using a bicinchoninic acid assay kit (Beyotime Institute of Biotechnology). Proteins (30 μg) were separated by SDS-PAGE on 12% gels and transferred to PVDF membranes. After blocking at room temperature for 20 min with protein-free blocking solution (Beyotime Institute of Biotechnology) and incubating overnight with antibodies against the target proteins at 4˚C, as follows: BCL2 (1:2,000; cat. no. ab182858; Abcam), BAX (1:2,000; cat. no. ab32503; Abcam), caspase 3 (1:5,000; cat. no. ab32351; Abcam), cleaved-caspase 3 (1:500; cat. no. ab32042; Abcam), PARP (1:1,000; cat. no. ab191217; Abcam), cleaved-PARP (1:1,000; cat. no. ab32561; Abcam), β-actin (1:500; cat. no. ab205; Abcam), CDK1 (1:10,000; cat. no. ab133327; Abcam), p-CDK1 (Thr161) (1:1,000; cat. no. ab47329; Abcam), p53 (1:1,000; cat. no. ab32049; Abcam), p-p53 (Ser315) (1:1,000; cat. no. WL02504; Wanleibio Co., Ltd.). Horseradish peroxidase-conjugated AffiniPure goat anti-rabbit immunoglobulin G (IgG) (1:1,000; cat. no. A0277; Beyotime Institute of Biotechnology) and goat anti-mouse IgG (1:1,000; cat. no. A0216; Beyotime Institute of Biotechnology) were used as the secondary antibody and incubated at room temperature for 1 h. Primary antibody diluent (cat. no. P0023A) and secondary antibody diluent (cat. no. P0023D) were from Beyotime Institute of Biotechnology. Subsequently, after adding an appropriate amount of electrochemiluminescence chromogenic substrate (BeyoECL Star; Beyotime Institute of Biotechnology), a chemiluminescence imaging system (GeneGnome XRQ; Syngene) was used to detect the chemiluminescence, and the intensity was measured using ImageJ software (1.54f; National Institutes of Health).

Inhibitors and activators. Ro3306 (cat. no. SC6673; Beyotime Institute of Biotechnology) was used as a CDK1 inhibitor at a working concentration of 20 nM. Pifithrin-α (pft-α; cat. no. S1816; Beyotime Institute of Biotechnology) was employed as a p53 phosphorylation inhibitor at a working concentration

of 10 μM. TC11 (cat. no. HY-129478; MedChemExpress) was used as a CDK1 activator at a concentration of 5 μM. These were dissolved in DMSO (cat. no. ST038; Beyotime Institute of Biotechnology). Briefly, after inducing THP-1 cells to differentiate into macrophages and adhere to the bottom of 6-well plates, the culture medium containing PMA was removed, and the same volume of fresh RPMI 1640 complete culture medium containing the aforementioned concentrations of the inhibitors and activator was added, followed by the addition of the bacterial solution for infection for 24 h at 37˚C and 5% CO_2.

Cell cycle analysis. The modeling of MTB cell infection was performed as described previously (using ~1x10^6 cells/well). Subsequently, the cells were collected, washed twice with PBS and fixed in 70% ethanol at 4˚C for 24 h. The cells were then stained with 500 μl propidium iodide/RNase staining buffer (BD Biosciences) at 37˚C for 15 min and cell cycle progression was detected by flow cytometry (BD FACSVerse; BD Biosciences). FlowJo (10.0.7r2; BD Biosciences) was used to analyze the results.

Apoptosis analysis. The apoptosis detection kit (cat. no. 556547; BD Biosciences) was used to assess the apoptosis of THP-1 cells. The modeling of MTB cell infection was performed as described previously (using ~1x10^6 cells/well). Briefly, the cells were collected, washed twice with pre-cooled PBS, and resuspended in 1X binding buffer. Subsequently, a 100-μl cell suspension (~1x10^5 cells) was incubated with 5 μl Annexin V-FITC and 5 μl propidium iodide at room temperature in the dark for 15 min, followed by resuspension in 400 μl 1X binding buffer and flow cytometry (BD FACSVerse; BD Biosciences). FlowJo (10.0.7r2) was used to analyze the results.

Co-immunoprecipitation (Co-IP). THP-1-derived macrophages infected with XJMTB were homogenized in 0.5% Triton X-100 (Beyotime Institute of Biotechnology) with 1X Halt™ Protease and Phosphatase Inhibitor SingleUse Cocktail (Thermo Fisher Scientific, Inc.). The cell lysate was centrifuged at 4˚C and 13,680 x g for 20 min to obtain a clear lysate. For IP, 5 μg rabbit IgG antibody (cat. no. HY-P80879; MedChemExpress), 5 μg rabbit CDK1 antibody (cat. no. HY-P80611; MedChemExpress) and 5 μg rabbit p53 antibody (cat. no. HY-P86169; MedChemExpress) were mixed with 500 μg protein solution, and incubated overnight at 4˚C. The protein A/G magnetic beads (Merck KGaA) were washed with 500 μl Cell Lysis Buffer for Western or IP (cat. no. P0013; Beyotime Institute of Biotechnology) three times. Afterwards, the mixture was mixed with 50 μl protein A/G magnetic beads and the antibody-protein A/G magnetic beads complex was gently shaken for 4 h at 4˚C, and 500 μl Cell Lysis Buffer for Western or IP was then added to the precipitate. The precipitate was then eluted with 100 μl 1X SDS loading buffer at 100˚C for 10 min. Finally, SDS-PAGE was performed with eluent and whole cell lysate (input), and western blotting was conducted as aforementioned.

Survival analysis of MTB in cells. Briefly, XJMTB-infected macrophage specimens were prepared according to the aforementioned method. The XJMTB specimens were washed with PBS to remove the extracellular bacteria. Subsequently, PBS containing 0.5% Triton X-100 was added to the cell culture dish to lyse the XJMTB-infected macrophages, and PBS containing the lysate of XJMTB-infected macrophage was diluted for 10, 100, 1,000 and 10,000 times, and inoculated onto 7H10 agar plates. The plates were incubated at 37˚C for 2-3 weeks, after which the colonies were counted.

Statistical analysis. Each experiment was repeated three times. Data are presented as the mean ± SEM. Statistical comparisons were performed using two-way ANOVA or one-way ANOVA, followed by Tukey's post hoc test, or using unpaired Student's t-test. All statistical analyses were conducted using SPSS version 24.0 (IBM Corp.). $P<0.05$ was considered to indicate a statistically significant difference.

Results

Study subjects. The isolation results in the modified acidic Roche's medium are shown in Fig. 1A, and the results of acid-fast staining are shown in Fig. 1B. The specific information and sputum features of the 20 patients are shown in Table I, including 12 male patients and eight female patients, aged 25-57 years old, with a median age of 40 years old. All patients had no history of smoking or other lung diseases, and tested negative for HIV. As shown in Table I, among the 20 patients, samples were successfully isolated and amplified from 16 patients. After PNB and TCH medium identification, 13 of them were isolated as MTB. A previous study conducted multiple-locus variable-number tandem repeat analysis strain typing and cluster analysis on the strains isolated from 103 sputum samples collected in the epidemiological survey (29), and it was revealed that most of the MTB strains prevalent in Xinjiang belonged to the Beijing MTB family (29,36,37). Rao *et al* (38) reported that Beijing family strains have seven repeat fragments at the MIRU 26 site (the size of the seven repeated segments is ~642 bp); therefore, this locus can be used for rapid identification of Beijing family strains. Fig. S1A shows the agarose gel electrophoresis patterns of the 13 MTB samples isolated after PCR of the MIRU 26 site, and Fig. S1B shows the cluster analysis of all strains collected by the collaborative team during the aforementioned epidemiological investigation.

Infection with MTB leads to increased secretion of inflammatory cytokines and NO. The induction of NO and pro-inflammatory cytokines produced by macrophages infected with MTB can lead to DNA damage, oxidative stress and persistent inflammation (28). Therefore, the current study detected the secretion of the cytokines TNF-α, IL-1β, IL-6, IL-10 and IL-12 in macrophages infected with different MTB strains at 12, 24 and 36 h. As shown in Fig. 2, compared with those in the C group without any MTB infection, the secretion levels of these cytokines in the V and L groups were significantly increased in a dose-dependent manner. After comprehensively observing the secretion levels of cytokines at various time points, 24 h was ultimately selected as the infection time for subsequent experiments, since there was no significant difference in the secretion of most cytokines between 24 and 36 h after infection.

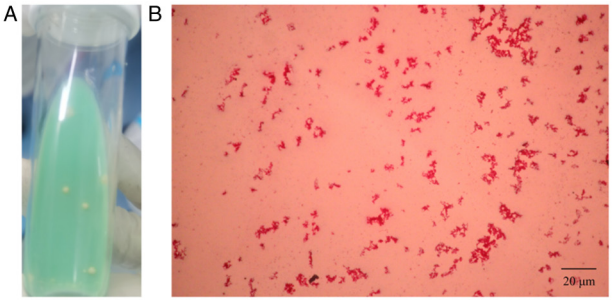

Figure 1. Isolation and acid-fast staining of *Mycobacterium tuberculosis*. (A) Results of isolation in modified acidic Roche's medium. (B) Acid-fast staining of an isolated *Mycobacterium tuberculosis* from Xinjang strain.

NO has a killing effect on MTB (39); therefore, the secretion of NO was assessed 24 h after infection. As shown in Fig. 2F, NO levels were lower in macrophages in the L group compared with those in macrophages in the V group, which may lead to enhanced survival of MTB in the L group.

CDK1 and cyclin A2 (CCNA2) expression levels are significantly elevated after MTB infection. To identify DEGs, transcriptome sequencing data between groups C, L and V were analyzed. The results showed that the expression levels of 2,848 mRNAs were significantly altered in the L group compared with the C group, of which 1,737 mRNAs were upregulated and 1,111 were downregulated (Fig. 3A and D). In group V compared with the C group, the expression levels of 1,678 mRNAs were significantly altered, with 1,011 upregulated and 667 downregulated mRNAs (Fig. 3B and E). The results of PCA between the three groups are shown in Fig. 3C. Furthermore, a Venn analysis was performed on the two sets of DEGs (Fig. 3F) and a follow-up analysis for the 1,527 DEGs between groups L and C was performed, since these unique 1,527 DEGs between groups L and C may reveal the specific biological processes triggered by XJMTB. GO term (Fig. 3G-I) and KEGG pathway (Fig. 3J) enrichment analyses revealed that multiple biological functions and pathways enriched by the 1,527 DEGs were associated with MTB infection, such as 'DNA conformation change' (40), 'phagocytic vesicle' (41), 'phagocytic vesicle membrane' (42), 'exonuclease activity' (43), 'endocytosis' (44,45), 'neutrophil extracellular trap formation' (46-48), 'cellular senescence' (49,50), 'natural killer cell mediated cytotoxicity' (51), 'p53 signaling pathway' (28,52) and 'nucleotide excision repair' (53).

To further explore the functions of the 1,527 mRNAs at the protein level, a PPI network (high confidence, 0.7) was established based on the results of the STRING database analysis, which consisted of 1,382 nodes and 14,264 edges. Subsequently, the plug-in MCODE in Cytoscape was used to deeply analyze the network, and the top module (score=29) was selected for subsequent research (Fig. 3K). The 33 mRNAs contained in this top module were regarded as critical mediators, and a functional analysis was performed. GO functional enrichment analysis showed that the 33 critical mediators were closely associated with 'cell mitosis' and the 'cell cycle' (Fig. 3L-N). R (3.6.3) software was applied to analyze the core genes in the PPI formed by the 1,527 genes. The top two genes were found to be CDK1 and CCNA2, and these genes were also found in the 33 key mRNAs. It has previously been shown that CDK1 and CCNA2 are closely related to the cell cycle (54). Furthermore, the previous GO and KEGG enrichment analyses showed that the unique 1,527 DEGs between groups L and C were enriched in terms of 'DNA replication' and other cell cycle related terms and pathways. Subsequently, RT-qPCR was used to detect the mRNA expression levels of CDK1 and CCNA2 (Fig. 3P), which showed significant differences between the L and C groups. Given that the mRNA expression levels of CDK1 in each group were consistent with the results of the bioinformatics analysis, and that the number of interaction nodes between CDK1 and other genes ranked first in Fig. 3O, CDK1 was identified as the target gene for subsequent studies.

Inhibition of CDK1 alleviates G_2/M cell cycle block and apoptosis caused by MTB infection. CDK1 is an enzyme necessary for initiating mitosis after the end of S-phase, and it can regulate the G_2/M checkpoint (17) and is closely related to apoptosis (18). Therefore, flow cytometry was performed to detect differential changes in the cell cycle of macrophages before and after infection with different sources of MTB. As shown in Fig. 4A-F, compared with in group C, groups V and L exhibited significantly higher G_2/M cell cycle blockage, and the ratio of cell cycle blockage was significantly higher in groups L3-5 than that in in group V, suggesting that macrophages infected with MTB could trigger G_2/M cell cycle block and that different sources of MTB could induce distinct degrees of cell cycle arrest. Notably, macrophages infected with XJMTB may trigger a more severe G_2/M cell cycle block compared with those infected with H37Rv.

The current study next examined the apoptosis of macrophages after infection with different sources of MTB using western blotting and flow cytometry. Compared with those in group C, the protein expression levels of BCL2 were decreased in groups L and V, whereas the protein expression levels of BAX and cleaved-caspase 3 (Fig. 4G and H), and cleaved-PARP (Fig. S2) were increased. Compared with that in group C (Fig. 4I), groups V (Fig. 4J) and L (Fig. 4K-M) exhibited marked apoptosis, with the degree of apoptosis being significantly stronger in group L than that in group V (Fig. 4N). These findings suggested that MTB could induce macrophage apoptosis, but the degree of macrophage apoptosis after infection with different sources of MTB varied, with the proportion of apoptotic macrophages infected with XJMTB being higher compared with those infected with H37Rv.

Next, the CDK1 inhibitor Ro3306 was used to inhibit the expression of CDK1 in macrophages after infection with different sources of MTB. The expression of CDK1 was first detected in group L before and after the addition of Ro3306, as shown in Fig. 5A and B. The findings indicated that the working concentration provided in the Ro3306 manual could effectively inhibit the expression of CDK1. The results of the flow cytometric analysis showed that the percentages of G_2/M cell cycle arrest in macrophages in the V group (Fig. 5C and G), L3 group (Fig. 5D and H), L4 group (Fig. 5E and I) and L5 group (Fig. 5F and J) were significantly decreased after the addition of Ro3306 (Fig. 5S). These results suggested that inhibiting CDK1 expression could attenuate the G_2/M cell cycle block of macrophages caused by infection with MTB.

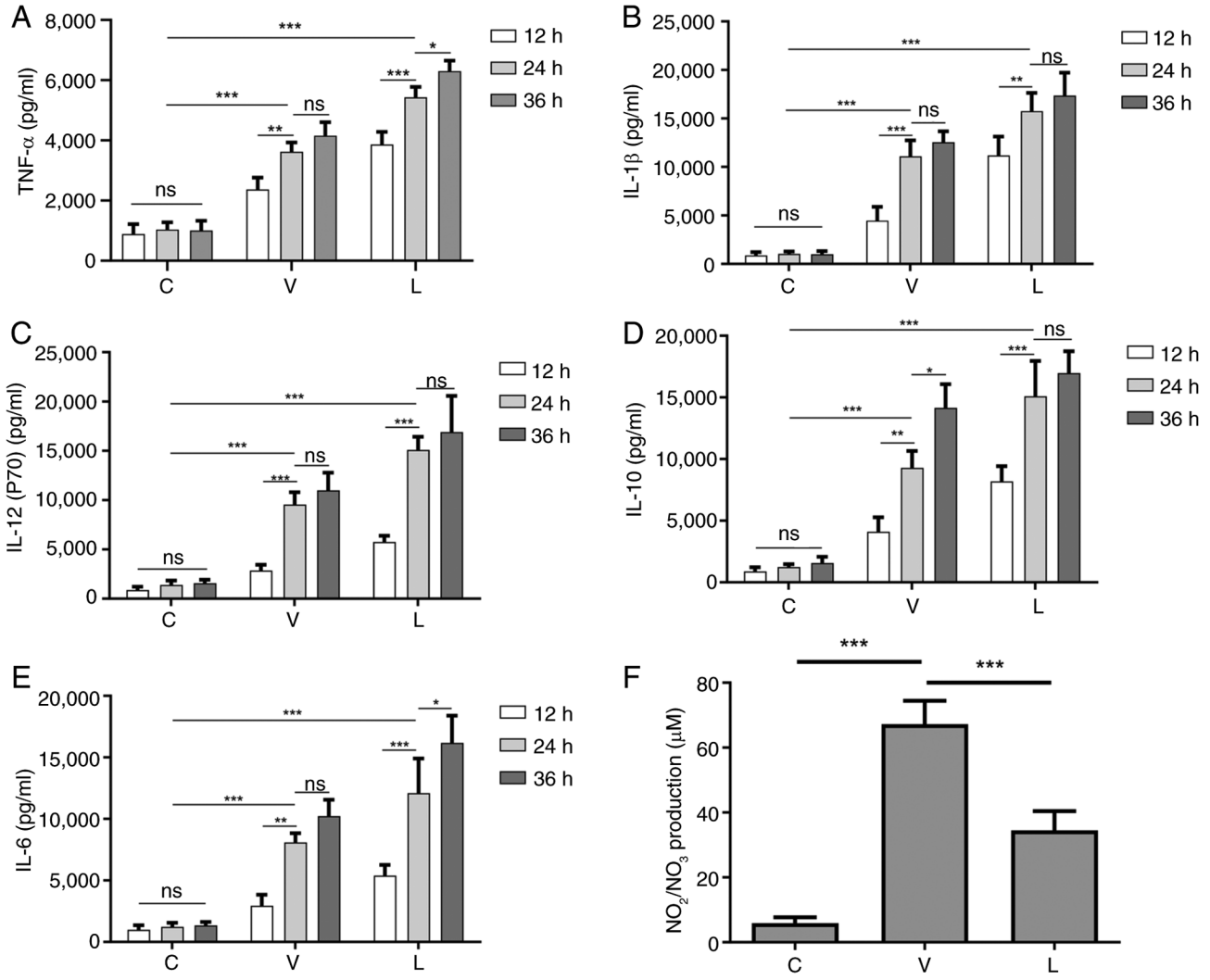

Figure 2. Secretion levels of cytokines at different time points after MTB infection of macrophages and the secretion level of NO 24 h after infection. Levels of (A) TNF-α, (B) IL-1β, (C) IL-12 (p70), (D) IL-10 and (E) IL-6 secretion at different time points after MTB infection in macrophages. (F) Levels of NO secretion in macrophages infected with MTB for 24 h. Data are presented as the mean ± SEM. *P<0.05, **P<0.01, ***P<0.001. C group, blank control group not infected with any bacteria; L group, MTB from Xinjang clinical isolate-infected group; MTB, *Mycobacterium tuberculosis*; NO, nitric oxide; ns, not significant; V group, H37Rv standard strain-infected group.

Similarly, the effects of the CDK1 inhibitor Ro3306 on macrophage apoptosis were examined after infection with different sources of MTB. The results of flow cytometry showed that the percentages of apoptotic macrophages in the V group (Fig. 5K and O), L3 group (Fig. 5L and P), L4 group (Fig. 5M and Q) and L5 group (Fig. 5N and R) were significantly decreased after the addition of Ro3306 (Fig. 5T). Furthermore, the results of western blotting showed that the protein expression levels of BCL2 were increased by Ro3306, whereas the protein expression levels of BAX and cleaved-caspase 3 (Fig. 5U and V), and cleaved-PARP (Fig. S3) were decreased. These findings suggested that inhibiting CDK1 expression could attenuate macrophage apoptosis caused by MTB infection.

The aforementioned results indicated that macrophages infected with MTB could induce G_2/M cell cycle block and apoptosis, but the degree of cell cycle arrest and apoptosis induced by different sources of MTB varied. The proportion of G_2/M cell cycle block and apoptosis in macrophages infected with XJMTB was significantly higher compared with that in macrophages infected with H37Rv. Furthermore, the degree of apoptosis and G_2/M cell cycle arrest in macrophages infected with H37Rv or XJMTB was alleviated after inhibiting CDK1 expression, which was consistent with the predicted result of the bioinformatics analyses, suggesting that CDK1 may be a key regulatory gene for G_2/M cell cycle arrest and apoptosis in macrophages with MTB infection.

Inhibition of p53 (Ser315) phosphorylation attenuates G_2/M cell cycle arrest and apoptosis caused by MTB infection. Since the 'p53 signaling pathway' was revealed to be enriched in the aforementioned KEGG analysis, and it is well known that CDK1 can interact with p53 to affect cell cycle progression and apoptosis (55), the current study examined the expression of p53 in macrophages after infection with different sources of MTB. As shown in Fig. 6A and B, the expression levels of p53 were significantly elevated after infection with different sources of MTB, but there was no significant difference between the two infection groups, suggesting that the G_2/M cell cycle arrest and apoptosis caused by high expression

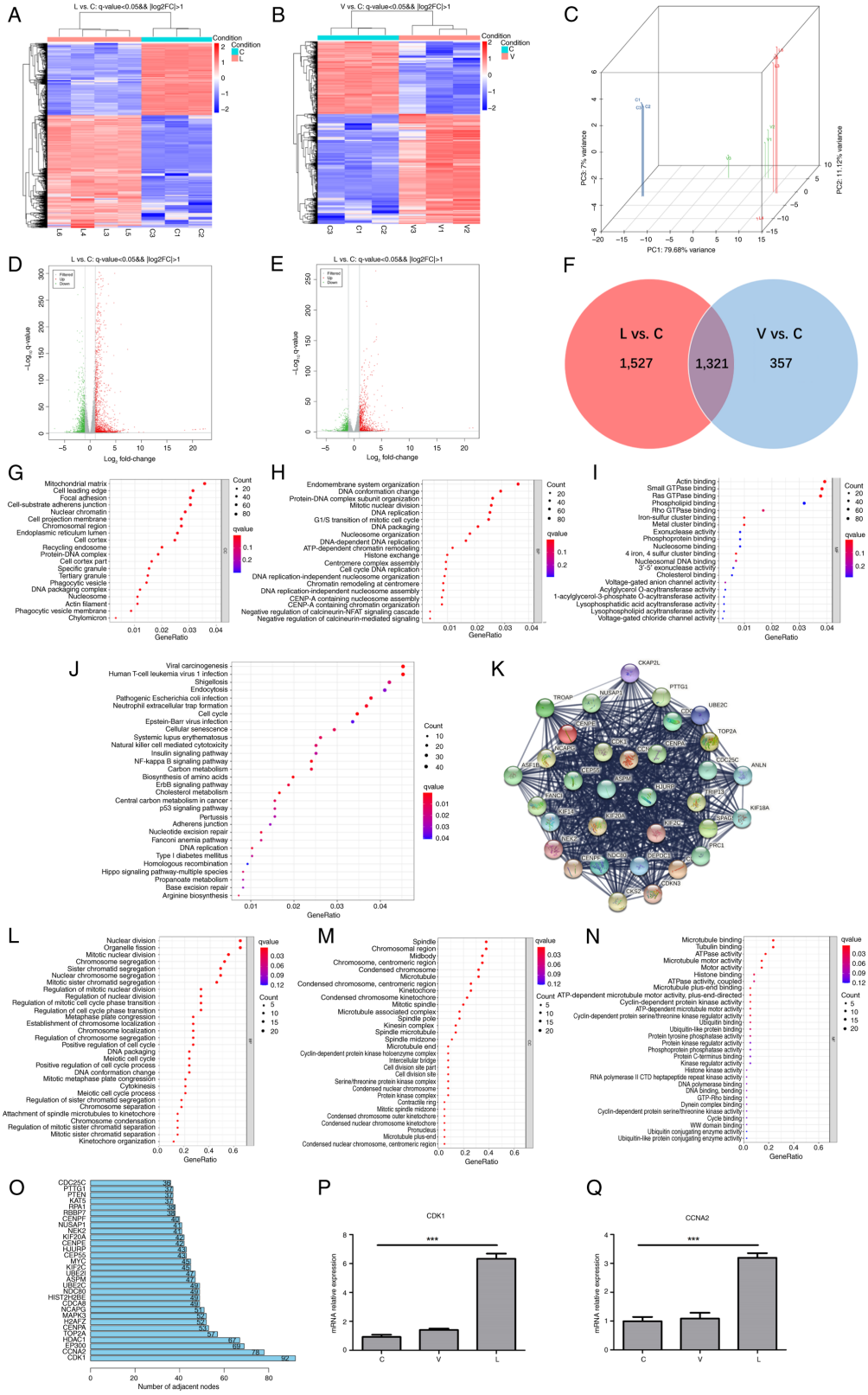

Figure 3. CDK1 expression is upregulated in response to infection with MTB. Heatmap of DEGs in (A) L and (B) V groups vs. C group. Red, high expression; blue, low expression. (C) Principal component analysis of group L, group V and group C. Volcano plots of DEGs in the (D) L and (E) V groups (|log2 fold change|≥1; P<0.05). Green, downregulated expression; gray, no differential expression; red, upregulated expression. (F) Venn diagram of L vs. C DEGs and V vs. C DEGs. GO functional enrichment analysis of 1,527 mRNAs: (G) Cellular components, (H) biological processes and (I) molecular functions. (J) Kyoto Encyclopedia of Genes and Genomes pathway enrichment analysis of 1,527 mRNAs. (K) Protein-protein interaction network top-level module containing 35 genes modularized by the plug-in MCODE. GO functional enrichment analysis of 35 key mRNAs: (L) Biological processes, (M) cellular components and (N) molecular functions. (O) Top 30 genes of the 1,527 mRNAs contained in the module that interacted most closely with other genes in the module. Expression of (P) CDK1 and (Q) CCNA2 in each group was verified through reverse transcription-quantitative polymerase chain reaction. Data are presented as the mean ± SEM. ***P<0.001. C group, blank control group not infected with any bacteria; CCNA2, cyclin A 2; CDK1, cyclin-dependent kinase; DEG, differentially expressed gene; GO, Gene Ontology; L group, MTB from Xinjang clinical isolate-infected group; MTB, *Mycobacterium tuberculosis*; V group, H37Rv standard strain-infected group.

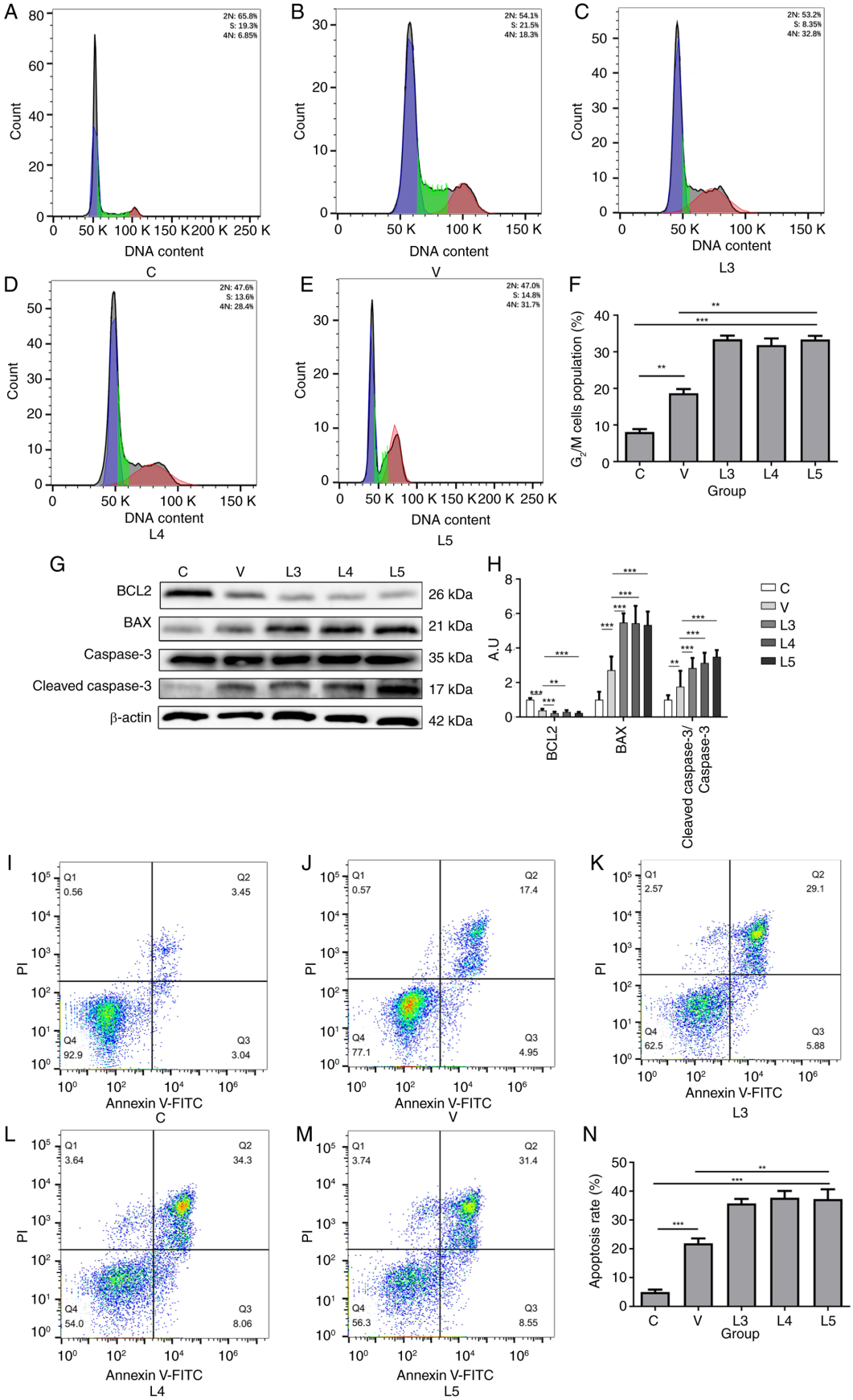

Figure 4. Infection with XJMTB causes stronger G_2/M cell cycle arrest and apoptosis than infection with H37Rv. Cell cycle profile of macrophages in the (A) C group, (B) V group, (C) L3 group, (D) L4 group and (E) L5 group. (F) G_2/M cell cycle ratio in each group. (G) Protein expression levels of BCL2, BAX, BCL-2, caspase 3 and cleaved-caspase 3 were determined by western blotting. (H) Statistical analysis of apoptosis-related proteins detected by western blotting. Apoptosis of macrophages in the (I) C group, (J) V group, (K) L3 group, (L) L4 group and (M) L5 group. (N) Apoptosis rate in each group. Data are presented as the mean ± SEM. **P<0.01, ***P<0.001. A.U., arbitrary units; C group, blank control group not infected with any bacteria; L group, XJMTB clinical isolate-infected group; MTB, *Mycobacterium tuberculosis*; V group, H37Rv standard strain-infected group; XJMTB, MTB from Xinjang.

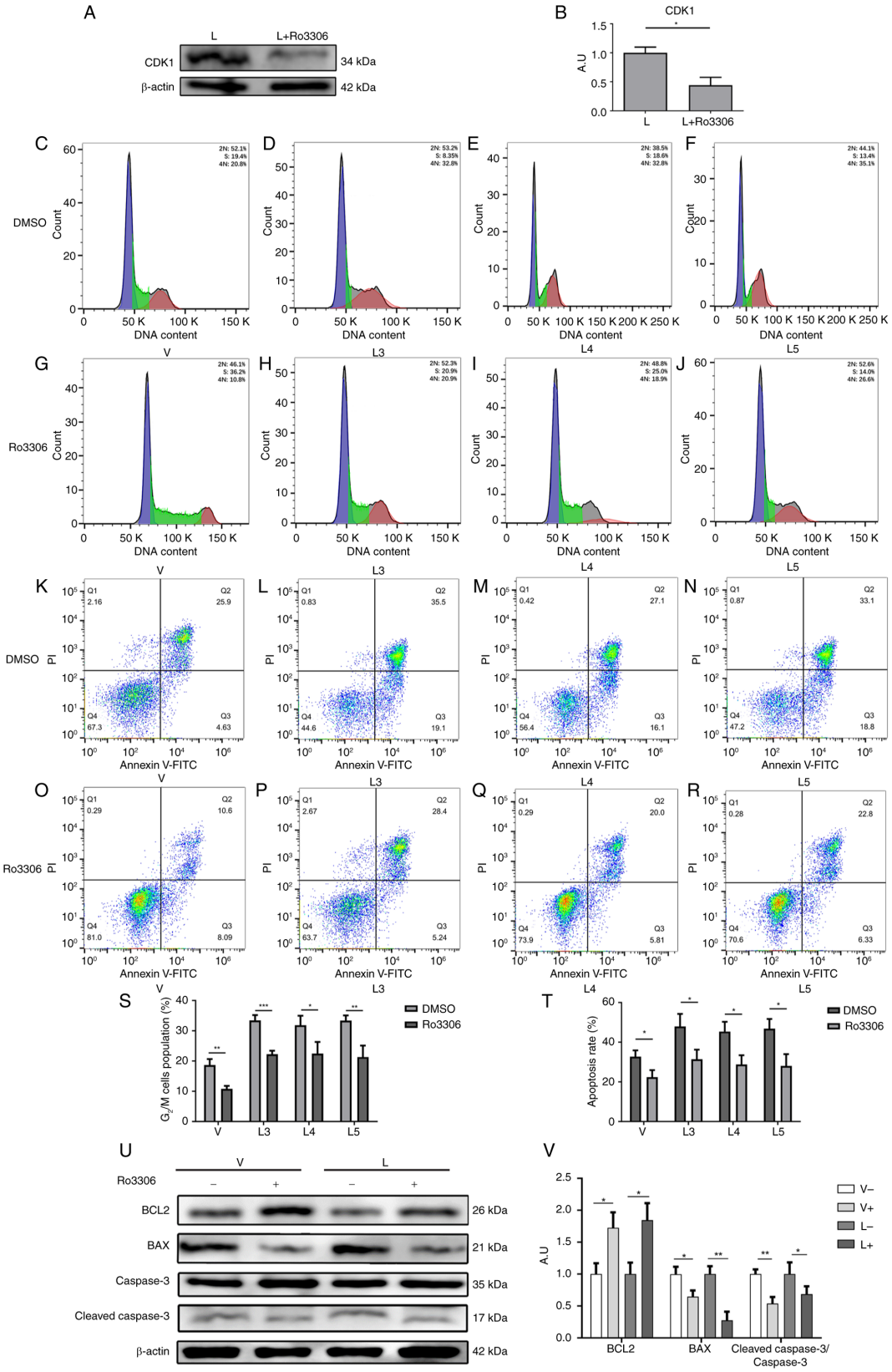

Figure 5. Inhibition of CDK1 alleviates macrophage G_2/M cycle arrest and apoptosis caused by MTB infection. (A) Protein expression levels of CDK1 were determined by western blotting. (B) Statistical analysis of CDK1 protein expression detected by western blotting. Cell cycle profiles of macrophages in the (C) V group, (D) L3 group, (E) L4 group and (F) L5 group when Ro3306 was not added. Cell cycle profiles of macrophages in the (G) V group, (H) L3 group, (I) L4 group and (J) L5 group after the addition of Ro3306. Apoptosis of macrophages in the (K) V group, (L) L3 group, (M) L4 group and (N) L5 group when Ro33006 was not added. Apoptosis of macrophages in the (O) V group, (P) L3 group, (Q) L4 group and (R) L5 group after the addition of Ro3306. (S) G_2/M cell cycle ratio and (T) apoptosis rate in each group before and after the addition of Ro3306. (U) Protein expression levels of BCL2, BAX, Bcl-2, caspase 3 and cleaved-caspase 3 were determined by western blotting before and after the addition of Ro3306. (V) Statistical analysis of apoptosis-related protein expression detected by western blotting before and after the addition of Ro3306. Data are presented as the mean ± SEM. *P<0.05, **P<0.01, ***P<0.001. A.U., arbitrary units; CDK1, cyclin-dependent kinase; L group, MTB from Xinjang clinical isolate-infected group; MTB, *Mycobacterium tuberculosis*; V group, H37Rv standard strain-infected group.

of CDK1 after MTB infection was not achieved by directly affecting p53 expression.

Fogal *et al* (56) demonstrated that CDK1 could mediate the phosphorylation of p53 at the Ser315 site to affect apoptosis, and indicated that the expression of total p53 may not change during this process. Therefore, the present study examined the phosphorylation of p53 at the Ser315 site in macrophages infected with different sources of MTB. The results showed that the phosphorylation of p53 at the Ser315 site was higher in macrophages infected with XJMTB than in those infected with H37Rv (Fig. 6A and B), suggesting that the G2/M cell cycle arrest and apoptosis caused by high expression of CDK1 after infection with MTB might be mediated by the phosphorylation of p53 at the Ser315 site.

Subsequently, the p53 inhibitor pft-α was used to inhibit the phosphorylation of p53. The expression of p53 and the phosphorylation of p53 (Ser315) before and after the addition of pft-α is shown in Fig. 6C and D. The findings indicated that the working concentration recomeded in the pft-α instruction manual could effectively inhibit the phosphorylation of p53 (Ser315). The results of flow cytometric analysis revealed that the percentages of G_2/M cell cycle block in macrophages in the V group (Fig. 6E and I), L3 group (Fig. 6F and J), L4 group (Fig. 6G and K) and L5 group (Fig. 6H and L) were decreased after the addition of pft-α (Fig. 6U). These findings indicated that inhibiting the phosphorylation of p53 (Ser315) could attenuate the G_2/M cell cycle arrest caused by MTB infection.

The current study then examined the effect of pft-α on the apoptosis of macrophages after infection with different sources of MTB. The results of flow cytometric analysis showed that the percentages of apoptotic macrophages in the V group (Fig. 6M and Q), L3 group (Fig. 6N and R), L4 group (Fig. 6O and S) and L5 group (Fig. 6P and T) were decreased after the addition of pft-α (Fig. 6V). The western blot analysis showed that the protein expression levels of BCL2 were increased after the addition of pft-α, whereas the protein expression levels of BAX and cleaved-caspase 3 (Fig. 6W and X), and cleaved-PARP (Fig. S4) were decreased. The two experiments suggested that inhibiting the phosphorylation of p53 (Ser315) could attenuate macrophage apoptosis due to infection with MTB.

The aforementioned results indicated that infection with MTB could induce elevated p53 expression; however, there was no significant difference in p53 expression among macrophages infected with different sources of MTB, whereas there was a difference in the phosphorylation of p53 (Ser315). The degree of macrophage apoptosis and G_2/M cell cycle arrest caused by infection with different sources of MTB was alleviated by inhibiting the phosphorylation of p53 (Ser315), which was consistent with the predicted result of the bioinformatics analysis, suggesting that p-p53 may be a key regulatory protein for G_2/M cell cycle block and apoptosis in macrophages infected with MTB. Therefore, it was hypothesized that a regulatory relationship may exist between CDK1 and p-p53.

Effect of inhibiting CDK1 expression or p53 (Ser315) phosphorylation on cytokine and NO secretions in MTB-infected macrophages. The present study revealed that the secretion levels of TNF-α, IL-6, IL-12, IL-10 and IL-1β were increased after MTB infection of macrophages. Therefore, the secretions of TNF-α, IL-6, IL-12, IL-10, IL-1β and NO were examined before and after inhibiting CDK1 expression or p53 (Ser315) phosphorylation. As shown in Fig. 7, in macrophage models infected with MTB from different sources, inhibition of CDK1 expression (MTB + Ro3306) or p53 (Ser315) phosphorylation (MTB + Pft-α) resulted in a significant decrease in the secretion of TNF-α, IL-6, IL-12, IL-10 and IL-1β, but no change in NO secretion. These results indicated that inhibiting CDK1 expression or p53 (Ser315) phosphorylation may suppress the release of inflammatory cytokines in THP-1-derived macrophages infected with MTB.

CDK1 mediates G_2/M cell cycle arrest and apoptosis induced by MTB infection and MTB survival in macrophages by regulating p53 (Ser315) phosphorylation. To verify whether CDK1 could affect G_2/M cell cycle arrest and apoptosis due to MTB infection by regulating the phosphorylation of p53 (Ser315), western blotting was performed to examine the phosphorylation of p53 (Ser315) following the addition of Ro3306 to XJMTB-infected macrophages to inhibit the expression of CDK1. As shown in Fig. 8A and D, after the addition of Ro3306, the phosphorylation of p53 (Ser315) was subsequently decreased.

Subsequently, TC11 (an activator of CDK1) was used to activate CDK1. TC11 functions as a phenylacetylamide derivative and is structurally related to immunomodulatory active drugs, such as thalidomide, lenalidomide and pomalidomide (57). TC11 can induce MCL1 degradation and activate caspase 9 and CDK1, leading to cell apoptosis (58,59). Fig. 8B and E showed that TC11 could enhance the phosphorylation of CDK1 (Thr161), and the phosphorylation of p53 (Ser315) was also increased. Moreover, inhibiting the phosphorylation of p53 (Ser315) did not alter CDK1 expression (Fig. 8C and F). Therefore, it was hypothesized that CDK1 could regulate p53 (Ser315) phosphorylation in macrophages infected with XJMTB.

Next, cell cycle progression and apoptosis were examined in three situations: i) Activation of CDK1 only; ii) inhibition of p53 (Ser315) phosphorylation only; iii) and activation of CDK1 + inhibition of p53 (Ser315) phosphorylation. The aforementioned results revealed that elevated CDK1 expression and enhanced p53 phosphorylation levels led to G_2/M cell cycle arrest. TC11 can activate CDK1, whereas pft-α can inhibit p53 (Ser315) phosphorylation. The results of flow cytometry showed that the proportion of G_2/M cell cycle arrest in macrophages with CDK1 activation and p-p53 (Ser315) inhibition (Fig. 8I) was higher than that in macrophages with p-p53 (Ser315) inhibition alone (Fig. 8H), but lower than that in those with CDK1 activation (Fig. 8J). These findings indicated that the inhibitory ability of pft-α on p53 (Ser315) phosphorylation was weakened by TC11, thus suggesting that the CDK1 activation caused by TC11 could reverse the reduction in the proportion of G_2/M cell cycle block caused by the inhibition of p53 (Ser315) phosphorylation in macrophages infected with XJMTB.

As expected, flow cytometry results showed that the proportion of apoptosis in macrophages in which CDK1 was activated and p53 phosphorylation was inhibited (Fig. 8M) was higher than that in macrophages in which only p53 phosphorylation was inhibited (Fig. 8L), but lower than that

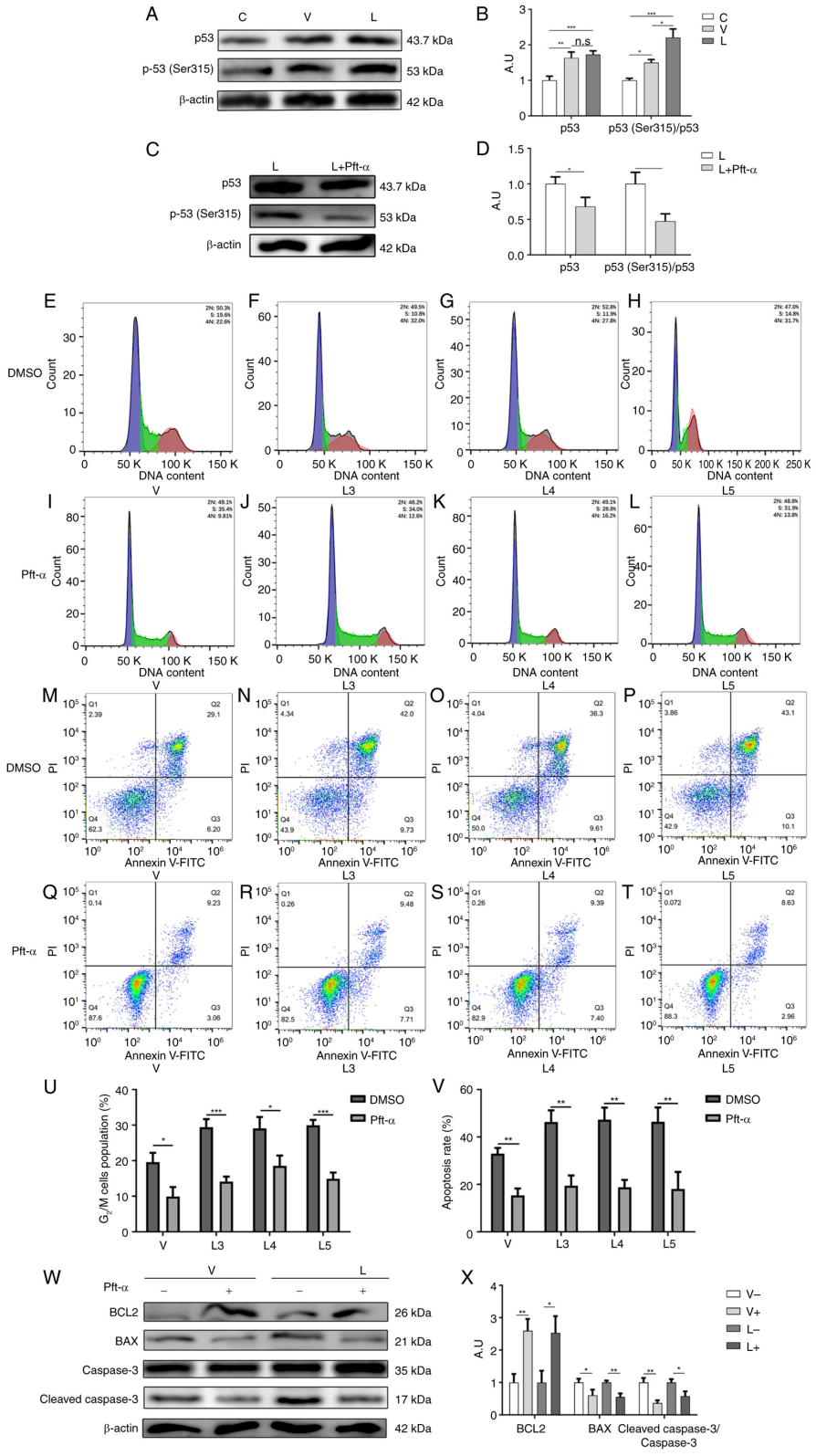

Figure 6. Inhibition of p53 (Ser315) phosphorylation attenuates macrophage G_2/M cycle block and apoptosis caused by MTB infection. (A) Protein expression levels of total p53 and p-p53 (Ser315) after MTB infection were determined by western blotting. (B) Statistical analysis of total p53 and p-p53 (Ser315) expression detected by western blotting after MTB infection. (C) Protein expression levels of total p53 and p-p53 (Ser315) were determined by western blotting before and after the addition of Pft-α. (D) Statistical analysis of total p53 and p-p53 (Ser315) expression determined by western blotting before and after the addition of Pft-α. Cell cycle profiles of macrophages in the (E) V group, (F) L3 group, (G) L4 group and (H) L5 group when Pift-α was not added. Cell cycle profiles of macrophages in the (I) V group, (J) L3 group, (K) L4 group and (L) L5 group after the addition of Pft-α. Apoptosis of macrophages in the (M) V group, (N) L3 group, (O) L4 group and (P) L5 group when Pft-α was not added. Apoptosis of macrophages in the (Q), V group, (R) L3 group, (S) L4 group and (T) L5 group after the addition of Pft-α. (U) G_2/M cell cycle ratio and (V) apoptosis rate of each group before and after the addition of Pft-α. (W) Protein expression levels of BCL2, BAX, caspase 3 and cleaved-caspase 3 were determined by western blotting before and after the addition of Pft-α. (X) Statistical analysis of apoptosis-related protein expression detected by western blotting before and after the addition of Pft-α. Data are presented as the mean ± SEM. *P<0.05, **P<0.01, ***P<0.001. A.U., arbitrary units; L group, MTB from Xinjang clinical isolate-infected group; MTB, *Mycobacterium tuberculosis*; n.s., not significant; p-, phosphorylated; Pft-α, pifithrin-α; V group, H37Rv standard strain-infected group.

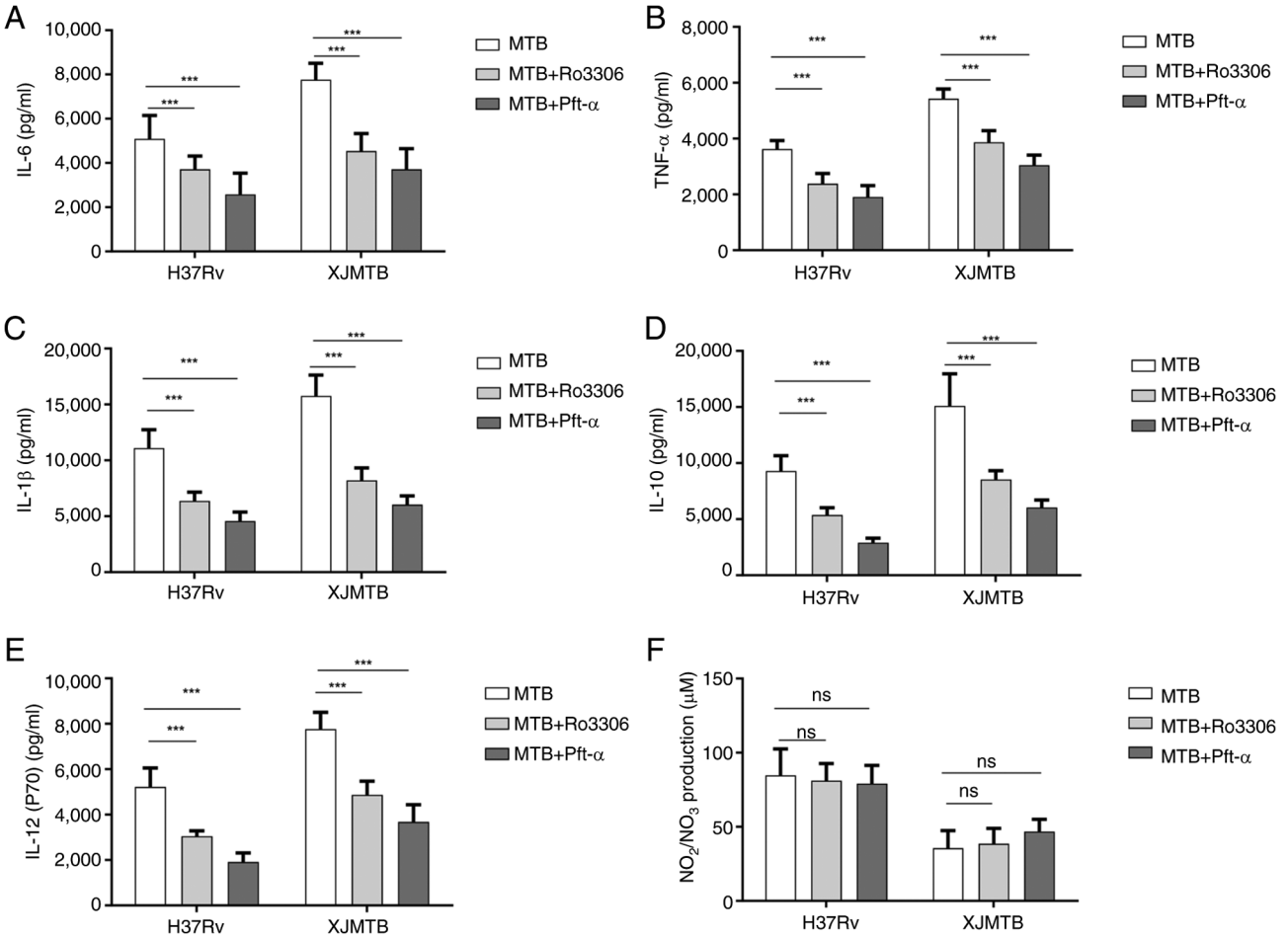

Figure 7. Secretion of cytokines and NO before and after inhibition of CDK1 expression or inhibition of p53 (Ser315) phosphorylation. Secretion of (A) IL-6, (B) TNF-α, (C) IL-1β, (D) IL-10, (E) IL-12 and (F) NO before and after inhibition of CDK1 expression or inhibition of p53 (Ser315) phosphorylation. Data are presented as the mean ± SEM. ***P<0.001. MTB, *Mycobacterium tuberculosis*; NO, nitric oxide; ns, not significant; Pft-α, pifithrin-α; XJMTB, MTB from Xinjang.

in macrophages in which only CDK1 was activated (Fig. 8K). Fig. 8N shows the apoptosis ratio in each group. Furthermore, the results of western blotting were consistent with those obtained by flow cytometry (Figs. 8O, P and S5). These findings suggested that TC11-induced CDK1 activation could reverse the reduction in the proportion of apoptosis caused by the inhibition of p53 (Ser315) phosphorylation in macrophages infected with XJMTB.

To clarify whether this regulatory relationship affected the survival of XJMTB in macrophages, XJMTB survival was assessed in macrophages under the aforementioned three conditions. As shown in Fig. 8Q, the survival rate of XJMTB in macrophages with CDK1 activation and p-p53 (Ser315) inhibition was higher than that in macrophages with p-p53 (Ser315) inhibition, but lower than that in those with CDK1 activation. These data strongly suggested that CDK1 activity influenced p53 phosphorylation levels.

To clarify the relationship between CDK1 and p53 in macrophages infected with XJMTB, Co-IP experiments were performed to observe whether they could interact with each other. The results showed that there was an interaction between CDK1 and p53 (Fig. 8R). CDK1 is a kinase that can transfer phosphate groups, thus it may be hypothesized that CDK1 can directly regulate p53 phosphorylation. Based on the aforementioned results in an *in vitro* model of XJMTB infected-macrophages, the high expression of CDK1 could enhance the phosphorylation of p53 (Ser315), affect the secretion of TNF-α, IL-6, IL-10, IL-1β and IL-12, promote G_2/M cell cycle arrest and apoptosis of macrophages, and enhance the survival of XJMTB in macrophages.

Discussion

TB is a complex disease involving multiple mechanisms (60), and macrophages are the first immune mechanism against MTB infection and the main effector cells to eliminate MTB (61). In the early stages of TB, MTB predominantly adopts an intracellular parasitic mode. The release of inflammatory factors (62), the production of reactive oxygen species (ROS) (63) and inducible NO synthase (iNOS) (62), and macrophage autophagy (64) and apoptosis (65) after MTB infection affect the ability of macrophages to clear MTB. However, their effects on the ability of macrophages to clear MTB is not very clear, especially autophagy and apoptosis. The morbidity of TB in Xinjiang is markedly higher than the national average (4), bringing great economic pressure to the majority of patients, and seriously affecting their physical and mental health. The search for specific immune responses

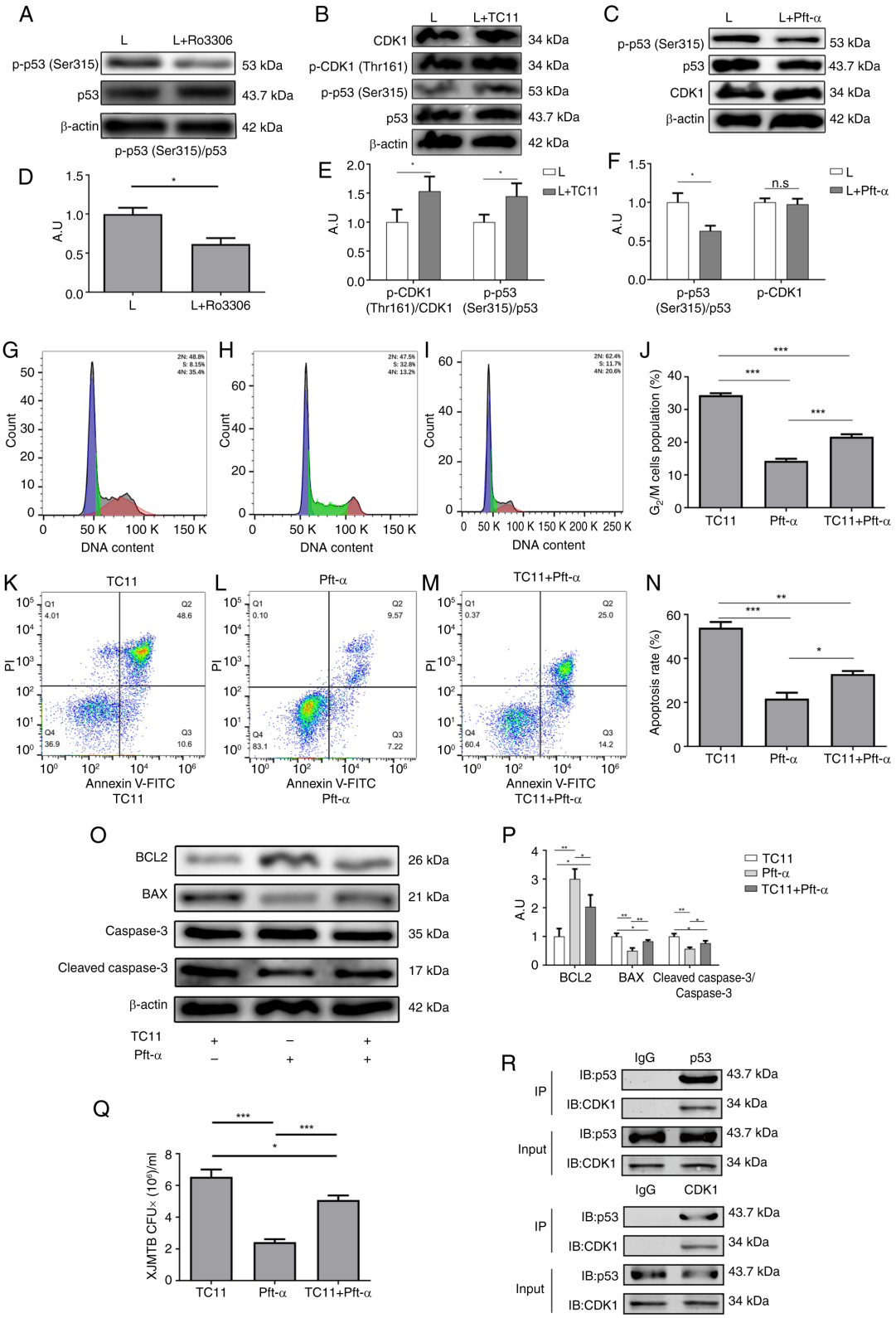

Figure 8. CDK1 mediates G_2/M cell cycle arrest and apoptosis caused by infection with XJMTB through regulation of p53 (Ser315) phosphorylation. (A) Phosphorylation of p53 (Ser315) after inhibition of CDK1. (B) Phosphorylation of CDK1 (Thr161) and of p53 (Ser315) following treatment with TC11. (C) Expression of CDK1 after inhibition of p53 (Ser315) phosphorylation. (D) Statistical analysis of total p53 and p-p53 (Ser315) expression determined by western blotting before and after the addition of Ro3306. (E) Statistical analysis of total p53, p-p53 (Ser315), total CDK1 and p-CDK1 (Thr161) expression determined by western blotting before and after the addition of TC11. (F) Statistical analysis of total p53, p-p53 (Ser315) and total CDK1 expressiondetermined by western blotting before and after the addition of Pft-α. Cell cycle progression of XJMTB-infected macrophages in the (G) TC11, (H) Pft-α and (I) TC11 + Pft-α groups. (J) G_2/M cell cycle ratio in the various groups. Apoptosis of XJMTB-infected macrophages in the (K) TC11, (L) Pft-α and (M) TC11 + Pft-α groups. (N) Apoptosis rate in the various groups. (O and P) Protein expression levels of BCL2, BAX, caspase 3 and cleaved-caspase 3 were determined by western blotting in the TC11, Pft-α and TC11 + Pft-α groups. (Q) CFU analysis was performed to determine the survival rate of XJMTB in macrophages in the TC11, Pft-α and TC11 + Pft-α groups. (R) Co-IP results of CDK1 and p53. Data are presented as the mean ± SEM. *P<0.05, **P<0.01, ***P<0.001. A.U., arbitrary units; CDK1, cyclin-dependent kinase; CFU, colony-forming unit; IB, immunoblotting; IgG, immunoglobulin G; IP, immunoprecipitation; L group, XJMTB clinical isolate-infected group; MTB, *Mycobacterium tuberculosis*; n.s., not significant; p-, phosphorylated; Pft-α, pifithrin-α; XJMTB, MTB from Xinjang.

triggered by XJMTB may help develop targeted control strategies for TB. Therefore, the present study used transcriptome sequencing to identify specific immune responses triggered by XJMTB.

Cell cycle progression is tightly regulated by cyclins and their catalytic partners, CDKs (66-68). Cyclin and CDKs can regulate the progression of the G_1, S, G_2 and M phases of the cell cycle through various mechanisms, which may include periodic synthesis and degradation, post-translational modification and subcellular localization (69). Cyclins are a large class of proteins characterized by the presence of a CDK-binding domain called the 'cyclin box', of which the cell cycle regulator CCNA2 is a member. The results of the present bioinformatics analysis showed that the expression levels of CDK1 and CCNA2 were significantly elevated in macrophages infected with XJMTB compared with in those infected with H37Rv, suggesting that XJMTB could lead to more severe cell cycle arrest, affect macrophage proliferation and influence the effectiveness of the host immune defense. There have been numerous reports on the role of CDK1 in various diseases (70-74); however, to the best of our knowledge, no reports have described its role in TB. According to the present results, the number of interaction nodes between CDK1 and other genes ranked higher than CCNA2, and since kinases serve an important role in the post-translational modification of proteins CDK1 was selected as the primary research target.

Notably, the regulatory relationship between CDK1 and the cell cycle and apoptosis has been widely reported in a number of studies (18,75,76). The present findings suggested that elevated CDK1 expression in macrophages infected with MTB could lead to the exacerbation of G_2/M cell cycle block and a higher proportion of apoptotic cells. When the expression of CDK1 was inhibited by Ro3306, the proportion of G_2/M cell cycle block and macrophage apoptosis was reduced, suggesting that CDK1 may be essential in MTB infection-induced cell cycle arrest and apoptosis. It has previously been shown that p53 can promote cell cycle arrest, induce DNA repair, and participate in various cell death-related pathways and metabolic changes (77-79). Notably, macrophages infected with MTB have been shown to exhibit increased p53 (Ser315) phosphorylation and enhanced apoptosis (80). Similarly, the current study revealed that an increase in p53 (Ser315) phosphorylation led to G_2/M cell cycle arrest and apoptosis in MTB-infected macrophages. Yuan *et al* (81) showed that circular RNA CEA could promote CDK1-mediated phosphorylation of p53 at the Ser315 site, which was in line with the results of the present study, which revealed that elevated CDK1 expression could regulate p53 (Ser315) phosphorylation.

Infection with MTB leads to macrophage apoptosis (82-85), which may be mediated by surface or secreted proteins. MTB Rv3261 protein can induce ROS production to inhibit MTB growth in macrophages, activate caspase 3/9-dependent pathways, and induce macrophage apoptosis (86). Medha *et al* (87) showed that the C-terminal and N-terminal sequences of MTB Rv0335c were similar to those of the BCL2 protein, and *in vitro* experiments confirmed that it could lead to apoptosis. The present study observed elevated cleaved-caspase 3 expression and decreased BCL2 expression following infection with MTB, and this phenomenon was more pronounced in samples infected with XJMTB than in those infected with H37Rv.

There is a view that although apoptosis is usually a non-inflammatory form of cell death, excessive apoptosis may lead to the propagation of MTB, which is beneficial for the pathogen rather than the host (12,13). Host infection can be exacerbated by the elimination of important host defense cells, penetration of the epithelial barrier and transmission of pathogens to immature host phagocytes that engulf apoptotic bodies (88). It has been shown that Fas-mediated apoptosis does not affect the survival of macrophages and MTB (89). Kelly *et al* (90) showed that infected macrophages can induce apoptosis of uninfected macrophages in a cell-to-cell contact-dependent manner, leading to exacerbation of MTB infection. In addition, Lee *et al* (91) reported that bacteria released from apoptotic macrophages infected with MTB were still alive and could subsequently grow extracellularly. Furthermore, H37Rv has been reported to induce more cell death compared with H37Ra, and this mode of death was initially characterized by apoptosis (91-93). Gan *et al* (92) infected mice *in vivo* with the MTB H37Rv strain or attenuated H37Ra strain, and showed that H37Rv induced a higher macrophage death rate and notably depleted resident alveolar macrophages, whereas H37Ra resulted in a marked reduction in cell death and only partially depleted the resident macrophages. Afriyie-Asante *et al* (94) revealed that MTB inhibited ROS production by decreasing focal adhesion kinase expression, leading to apoptosis and persistent lung injury. One hypothesis is that apoptosis in the late stages of infection during granuloma formation may be a pathogenic process that increases the persistence and future spread of MTB (95). In addition, macrophage apoptosis caused by MTB may evolve into macrophage necrosis, which releases cellular contents and triggers inflammation (96,97), and sustained inflammation exacerbates tissue damage and leads to disease progression (98,99). Compared with other forms of cell death, apoptotic cells may be less likely to activate the specific immune responses required to control MTB infection (100). As aforementioned, H37Rv can induce more severe apoptosis than H37Ra, and H37Rv is more pathogenic than H37Ra. This is consistent with the present findings that XJMTB, which is more pathogenic, induces stronger macrophage apoptosis compared with H37Rv. Nevertheless, there is also a view that activating host cell apoptosis is an important defense strategy for pathogens that utilize host cell resources for survival and replication, meaning that the more severe the apoptosis, the better the bactericidal effect (101). Moreover, the virulence of MTB has been reported to be negatively associated with the degree of classical apoptosis, and the attenuated strain H37Ra has been suggested to induce more apoptosis compared with the highly virulent strain H37Rv (102).

The aforementioned studies suggest that the macrophage apoptosis induced by MTB infection can be beneficial for both the host and MTB, which may be influenced by the viability of the bacteria and host cells, as well as the duration of the infection (103). Therefore, it is hypothesized that apoptosis can be considered as having a dual role. Apoptosis is a means of controlling the growth of intracellular pathogens and is capable of killing MTB only under the appropriate conditions (89,104-108). The fate of cells may depend on the balance between pro- and anti-apoptotic signals emitted by the cell or pathogen, as well as other variables, including host

species, origin and state of the host cell differentiation, *in vitro* culture conditions, MTB strains and multiplicity of infection. MTB can induce macrophage apoptosis directly when objective conditions change (109), regardless of the killing effect of MTB (110). In addition, in the presence of large numbers of mycobacteria and when large numbers of apoptotic cells exceed the local phagocytic clearance capacity of macrophages, macrophages are considered to be critical for the clearance of apoptotic vesicles, and thus ineffective clearance of apoptotic cells may lead to tissue damage (111). Moreover, unabsorbed apoptotic cells may undergo secondary necrosis, thereby favoring MTB dissemination (112). These results suggest that when infected with MTB, the occurrence of massive apoptosis in macrophages does not necessarily represent notable clearance of MTB, but rather indicates an exacerbation of the infection, which explains the phenomenon that clinical isolates of XJMTB were more likely to induce macrophage apoptosis compared with clinical isolates of H37Rv.

NO is a free radical mediator that serves an important role in the immune system. Long *et al* (39) concluded that exogenous NO has a time- and dose-dependent killing effect on MTB, and that short-term exposure of extracellular MTB to low concentrations of NO (<100 ppm) can kill MTB. During macrophage infection, NO may act directly or combine with superoxide to form peroxynitrite, which kills MTB in phagosomes (113). NOS converts L-arginine to NO, which is protective against parasitic infections and a variety of infectious organisms, such as MTB (114,115). Mice deficient in iNOS have been shown to be highly susceptible to MTB infection, permitting MTB infection and leading to early death (116-118). Furthermore, the expression levels of iNOS are higher in the peripheral monocytes and alveolar macrophages of patients with TB compared with those in healthy individuals (119). These studies indicated that NO may have a strong bactericidal effect on MTB-infected macrophages. In the present study, XJMTB induced a lower secretion of NO than H37Rv, which may explain its enhanced survival in macrophages.

It has been shown that in the J774.1 macrophage model of mice infected with *Mycobacterium bovis* BCG, IFN-γ and lipopolysaccharide treatment enhance the expression of the arginine permease MCAT2B; however, this does not explain the observed increase in L-arginine uptake, suggesting that the activity of the L-arginine transporter may also be altered in response to macrophage activation, which in turn affects NO production (120). In addition, expression of the solute carrier family 11 member 1 gene affects the ability of macrophages to produce NO, resulting in differential susceptibility or resistance to MTB (121). NO production by alveolar macrophages in patients with TB may have an autoregulatory role, which can promote proinflammatory cytokine production through activation of the transcription factor NF-κB (122-124). Upregulation of the inhibitor of NF-κB has confirmed that the IκBα kinase-NF-κB signaling pathway enhances IFN-γ- and MTB lipoarabinomannan-induced iNOS promoter activity and NO expression (124). These studies suggested that NO production is regulated by multiple factors and does not come from a single source, which may be one of the reasons why the regulation of the CDK1-p53 axis had no effect on NO secretion in the current study.

One limitation of the present study is the relatively small sample size, with only four strains of XJMTB used for infection and sequencing, which may limit the generalizability of the findings. Additionally, the study was conducted using a single cell line, THP-1, which might not reflect the broader population. The use of human monocyte-derived macrophages may enhance the physiological relevance of the study. However, primary monocyte-derived macrophages are difficult to obtain and isolate. We previously considered validating the relevant conclusions in the RAW264.7 cell line, but considering that RAW264.7 cells are mouse-derived cells, this cell line was not used due to species differences between humans and mice. In addition, the conclusions should be verified in animal experiments; however, animal experiments related to TB require extremely stringent experimental conditions and environments.

CDK1 was the target of the present study due to its high bioinformatics score and verifiability, as well as its novelty in the field of MTB. The identification of the 'p53 signaling pathway' entry in the bioinformatics analysis process attracted clarification as to whether a regulatory relationship exists between CDK1 and p53 in the process of MTB infection of macrophages, thus the upstream molecules that regulate the high expression of CDK1 were overlooked. Future research should include larger and more diverse samples to validate these results, including validating this mechanism in MTBs from other regions.

The present study showed that MTB infection of macrophages resulted in high CDK1 expression and increased levels of p53 (Ser315) phosphorylation, and that the level of p53 (Ser315) phosphorylation increased with CDK1 activation, leading to increased macrophage G_2/M cell cycle arrest and apoptosis. Compared with H37Rv, XJMTB infection typically led to a greater elevation of CDK1 and p-p53. Furthermore, Co-IP analysis showed that there was indeed a protein interaction between CDK1 and p53. The activation of CDK1 could reverse the reduction of G_2/M cell cycle arrest and apoptosis caused by p-p53 inhibition. These results suggested that the increase in p53 (Ser315) phosphorylation in MTB-infected macrophages may be caused by elevated CDK1 expression. In an *in vitro* model of XJMTB-infected macrophages, high activation of CDK1 can enhance the phosphorylation of p53 (Ser315), affect the secretion of TNF-α, IL-6, IL-10, IL-1β and IL-12, promote G_2/M cell cycle arrest and apoptosis of macrophages, and enhance the survival of XJMTB in macrophages. These findings lay the foundation for formulating treatment strategies targeting the prognosis of TB in Xinjiang, China. Future studies should explore the potential of targeting CDK1 and p53 phosphorylation in clinical settings. Regulating the macrophage cycle or apoptosis by adjusting the activity of CDK1 or p53 may be considered a potential treatment for TB.

Acknowledgements

The authors would like to thank Ms. Jing Wang (Department of Respiratory Medicine, The Second Affiliated Hospital of Hainan Medical College) for their contribution to specimen collection.

Funding

The present study received funding from the National Natural Science Foundation of China (grant no. 81672109).

Availability of data and materials

The sequencing data generated in the present study may be found in the Gene Expression Omnibus database under accession number GSE275640 or at the following URL: https://www.ncbi.nlm.nih.gov/geo/query/acc.cgi?acc=GSE275640. The other data generated in the present study may be requested from the corresponding author.

Authors' contributions

BS, QM, ZZ and FL conceptualized the study. XJ, SL and FC collected the data in the study and conducted statistical analysis. FL acquired funding. BS, QM, LP, ZZ and FL designed the study. FL conducted project administration. ZZ and FL provided materials and resources for the study. BS, QM and LP conducted bioinformatics analysis using software. FL supervised the study. BS, LP and XJ validated the research results obtained. FC and ZZ visualized the content and data to be published. BS and ZZ conducted the initial draft writing. QiM and FL reviewed and edited the manuscript. BS and FL confirm the authenticity of all the raw data. All authors read and approved the final manuscript.

Ethics approval and consent to participate

All protocols performed in the present study were approved by the Ethics Committee of Jilin University (approval no. 2016-057; Changchun, China). Written informed consent for participation was obtained from the patients.

Patient consent for publication

Not applicable.

Competing interests

The authors declare that they have no competing interests.

References

1. Abdullah M, Humayun A, Imran M, Bashir MA and Malik AA: A bibliometric analysis of global research performance on tuberculosis (2011-2020): Time for a global approach to support high-burden countries. J Family Community Med 29: 117-124, 2022.
2. Li XX, Zhang H, Jiang SW, Liu XQ, Fang Q, Li J, Li X and Wang LX: Geographical distribution regarding the prevalence rates of pulmonary tuberculosis in China in 2010. Zhonghua Liu Xing Bing Xue Za Zhi 34: 980-984, 2013 (In Chinese).
3. Wubuli A, Xue F, Jiang D, Yao X, Upur H and Wushouer Q: Socio-demographic predictors and distribution of pulmonary tuberculosis (TB) in Xinjiang, China: A spatial analysis. PLoS One 10: e0144010, 2015.
4. Wang L, Zhang H, Ruan Y, Chin DP, Xia Y, Cheng S, Chen M, Zhao Y, Jiang S, Du X, *et al*: Tuberculosis prevalence in China, 1990-2010; a longitudinal analysis of national survey data. Lancet 383: 2057-2064, 2014.
5. He X, Cao M, Mahapatra T, Du X, Mahapatra S, Li Q, Feng L, Tang S, Zhao Z, Liu J and Tang W: Burden of tuberculosis in Xinjiang between 2011 and 2015: A surveillance data-based study. PLoS One 12: e0187592, 2017.
6. Anilkumar U and Prehn JHM: Anti-apoptotic BCL-2 family proteins in acute neural injury. Front Cell Neurosci 8: 281, 2014.
7. Behar SM, Divangahi M and Remold HG: Evasion of innate immunity by *Mycobacterium tuberculosis*: Is death an exit strategy? Nat Rev Microbiol 8: 668-674, 2010.
8. Deretic V and Wang F: Autophagy is part of the answer to tuberculosis. Nat Microbiol 8: 762-763, 2023.
9. Arnett E and Schlesinger LS: Live and let die: TB control by enhancing apoptosis. Immunity 54: 1625-1627, 2021.
10. Häcker G: Apoptosis in infection. Microbes Infect 20: 552-559, 2018.
11. Ashida H, Mimuro H, Ogawa M, Kobayashi T, Sanada T, Kim M and Sasakawa C: Cell death and infection: A double-edged sword for host and pathogen survival. J Cell Biol 195: 931-942, 2011.
12. Hirsch CS, Johnson JL, Okwera A, Kanost RA, Wu M, Peters P, Muhumuza M, Mayanja-Kizza H, Mugerwa RD, Mugyenyi P, *et al*: Mechanisms of apoptosis of T-cells in human tuberculosis. J Clin Immunol 25: 353-364, 2005.
13. Pagán AJ and Ramakrishnan L: Immunity and immunopathology in the tuberculous granuloma. Cold Spring Harb Perspect Med 5: a018499, 2014.
14. Malumbres M and Barbacid M: Cell cycle, CDKs and cancer: A changing paradigm. Nat Rev Cancer 9: 153-166, 2009.
15. Enserink JM and Kolodner RD: An overview of Cdk1-controlled targets and processes. Cell Div 5: 11, 2010.
16. Morgan DO: Cyclin-dependent kinases: Engines, clocks, and microprocessors. Annu Rev Cell Dev Biol 13: 261-291, 1997.
17. Huang R, Gao S, Han Y, Ning H, Zhou Y, Guan H, Liu X, Yan S and Zhou PK: BECN1 promotes radiation-induced G2/M arrest through regulation CDK1 activity: A potential role for autophagy in G2/M checkpoint. Cell Death Discov 6: 70, 2020.
18. Huang S, Xiao J, Wu J, Liu J, Feng X, Yang C, Xiang D and Luo S: Tizoxanide promotes apoptosis in glioblastoma by inhibiting CDK1 activity. Front Pharmacol 13: 895573, 2022.
19. Zhang Q, Chen L, Gao M, Wang S, Meng L and Guo L: Molecular docking and in vitro experiments verified that kaempferol induced apoptosis and inhibited human HepG2 cell proliferation by targeting BAX, CDK1, and JUN. Mol Cell Biochem 478: 767-780, 2023.
20. Xu G, Yan X, Hu Z, Zheng L, Ding K, Zhang Y, Qing Y, Liu T, Cheng L and Shi Z: Glucocappasalin induces G2/M-phase arrest, apoptosis, and autophagy pathways by targeting CDK1 and PLK1 in cervical carcinoma cells. Front Pharmacol 12: 671138, 2021.
21. Yang YJ, Luo S and Xu ZL: Effects of miR-490-5p targeting CDK1 on proliferation and apoptosis of colon cancer cells via ERK signaling pathway. Eur Rev Med Pharmacol Sci 26: 2049-2056, 2022.
22. Tong Y, Huang Y, Zhang Y, Zeng X, Yan M, Xia Z and Lai D: DPP3/CDK1 contributes to the progression of colorectal cancer through regulating cell proliferation, cell apoptosis, and cell migration. Cell Death Dis 12: 529, 2021.
23. Huang Y, Fan Y, Zhao Z, Zhang X, Tucker K, Staley A, Suo H, Sun W, Shen X, Deng B, *et al*: Inhibition of CDK1 by RO-3306 exhibits anti-tumorigenic effects in ovarian cancer cells and a transgenic mouse model of ovarian cancer. Int J Mol Sci 24: 12375, 2023.
24. Ozaki T and Nakagawara A: Role of p53 in cell death and human cancers. Cancers (Basel) 3: 994-1013, 2011.
25. Chen J: The cell-cycle arrest and apoptotic functions of p53 in tumor initiation and progression. Cold Spring Harb Perspect Med 6: a026104, 2016.
26. Zheng SJ, Lamhamedi-Cherradi SE, Wang P, Xu L and Chen YH: Tumor suppressor p53 inhibits autoimmune inflammation and macrophage function. Diabetes 54: 1423-1428, 2005.
27. Fischer M: Census and evaluation of p53 target genes. Oncogene 36: 3943-3956, 2017.
28. Lim YJ, Lee J, Choi JA, Cho SN, Son SH, Kwon SJ, Son JW and Song CH: M1 macrophage dependent-p53 regulates the intracellular survival of mycobacteria. Apoptosis 25: 42-55, 2020.
29. Gong X, Li Y, Yao L, Aynur M, Liu N, Wang L and Wang J: Preliminary study on genotype of *Mycobacterium tuberculosis* in some areas of Xinjiang by the multiple locus VNTR analysis. Chin J Lung Dis (Electronic Edition) 10: 304-308, 2017 (In Chinese).
30. Chinese Society of Tuberculosis, Chinese Medical Association: Guidelines for the Diagnosis and Treatment of Pulmonary Tuberculosis. Chin J Tuberc Respir Dis 24: 70-74, 2001 (In Chinese).
31. Kim D, Paggi JM, Park C, Bennett C and Salzberg SL: Graph-based genome alignment and genotyping with HISAT2 and HISAT-genotype. Nat Biotechnol 37: 907-915, 2019.
32. Ghosh S and Chan CKK: Analysis of RNA-seq data using tophat and cufflinks. Methods Mol Biol 1374: 339-361, 2016.
33. Anders S, Pyl PT and Huber W: HTSeq-a Python framework to work with high-throughput sequencing data. Bioinformatics 31: 166-169, 2015.

34. Bader GD and Hogue CWV: An automated method for finding molecular complexes in large protein interaction networks. BMC Bioinformatics 4: 2, 2003.
35. Livak KJ and Schmittgen TD: Analysis of relative gene expression data using real-time quantitative PCR and the 2(-Delta Delta C(T)) method. Methods 25: 402-408, 2001.
36. Zhang J, Mi L, Wang Y, Liu P, Liang H, Huang Y, Lv B and Yuan L: Genotypes and drug susceptibility of *Mycobacterium tuberculosis* Isolates in Shihezi, Xinjiang Province, China. BMC Res Notes 5: 309, 2012.
37. Yuan L, Mi L, Li Y, Zhang H, Zheng F and Li Z: Genotypic characteristics of *Mycobacterium tuberculosis* circulating in Xinjiang, China. Infect Dis (Lond) 48: 108-115, 2016.
38. Rao KR, Ahmed N, Srinivas S, Sechi LA and Hasnain SE: Rapid identification of *Mycobacterium tuberculosis* Beijing genotypes on the basis of the mycobacterial interspersed repetitive unit locus 26 signature. J Clin Microbiol 44: 274-277, 2006.
39. Long R, Jones R, Talbot J, Mayers I, Barrie J, Hoskinson M and Light B: Inhaled nitric oxide treatment of patients with pulmonary tuberculosis evidenced by positive sputum smears. Antimicrob Agents Chemother 49: 1209-1212, 2005.
40. Butala B, Busada M and Cormican D: Malignant hyperthermia: Review of diagnosis and treatment during cardiac surgery with cardiopulmonary bypass. J Cardiothorac Vasc Anesth 32: 2771-2779, 2018.
41. Fatima N, Upadhyay T, Ahmad F, Arshad M, Kamal MA, Sharma D and Sharma R: Particulate β-glucan activates early and delayed phagosomal maturation and autophagy within macrophage in a NOX-2 dependent manner. Life Sci 266: 118851, 2021.
42. Majeed M, Perskvist N, Ernst JD, Orselius K and Stendahl O: Roles of calcium and annexins in phagocytosis and elimination of an attenuated strain of *Mycobacterium tuberculosis* in human neutrophils. Microb Pathog 24: 309-320, 1998.
43. Nasir N and Kisker C: Mechanistic insights into the enzymatic activity and inhibition of the replicative polymerase exonuclease domain from *Mycobacterium tuberculosis*. DNA Repair (Amst) 74: 17-25, 2019.
44. Parveen N, Varman R, Nair S, Das G, Ghosh S and Mukhopadhyay S: Endocytosis of *Mycobacterium tuberculosis* heat shock protein 60 is required to induce interleukin-10 production in macrophages. J Biol Chem 288: 24956-24971, 2013.
45. Sachdeva K, Goel M and Sundaramurthy V: Heterogeneity in the endocytic capacity of individual macrophage in a population determines its subsequent phagocytosis, infectivity and subcellular trafficking. Traffic 21: 522-533, 2020.
46. Moreira-Teixeira L, Stimpson PJ, Stavropoulos E, Hadebe S, Chakravarty P, Ioannou M, Aramburu IV, Herbert E, Priestnall SL, Suarez-Bonnet A, *et al*: Type I IFN exacerbates disease in tuberculosis-susceptible mice by inducing neutrophil-mediated lung inflammation and NETosis. Nat Commun 11: 5566, 2020.
47. Kroon EE, Correa-Macedo W, Evans R, Seeger A, Engelbrecht L, Kriel JA, Loos B, Okugbeni N, Orlova M, Cassart P, *et al*: Neutrophil extracellular trap formation and gene programs distinguish TST/IGRA sensitization outcomes among *Mycobacterium tuberculosis* exposed persons living with HIV. PLoS Genet 19: e1010888, 2023.
48. Dang G, Cui Y, Wang L, Li T, Cui Z, Song N, Chen L, Pang H and Liu S: Extracellular sphingomyelinase Rv0888 of *Mycobacterium tuberculosis* contributes to pathological lung injury of mycobacterium smegmatis in mice via inducing formation of neutrophil extracellular traps. Front Immunol 9: 677, 2018.
49. Bobak CA, Abhimanyu, Natarajan H, Gandhi T, Grimm SL, Nishiguchi T, Koster K, Longlax SC, Dlamini Q, Kahari J, *et al*: Increased DNA methylation, cellular senescence and premature epigenetic aging in guinea pigs and humans with tuberculosis. Aging (Albany NY) 14: 2174-2193, 2022.
50. Parandhaman DK and Narayanan S: Cell death paradigms in the pathogenesis of *Mycobacterium tuberculosis* infection. Front Cell Infect Microbiol 4: 31, 2014.
51. Li S, Wang D, Wei P, Liu R, Guo J, Yang B, Zhang H, Lu J, Gao M and Pang Y: Elevated natural killer cell-mediated cytotoxicity is associated with cavity formation in pulmonary tuberculosis patients. J Immunol Res 2021: 7925903, 2021.
52. Liang S, Song Z, Wu Y, Gao Y, Gao M, Liu F, Wang F and Zhang Y: MicroRNA-27b modulates inflammatory response and apoptosis during *Mycobacterium tuberculosis* infection. J Immunol 200: 3506-3518, 2018.
53. Houghton J, Townsend C, Williams AR, Rodgers A, Rand L, Walker KB, Böttger EC, Springer B and Davis EO: Important role for *Mycobacterium tuberculosis* UvrD1 in pathogenesis and persistence apart from its function in nucleotide excision repair. J Bacteriol 194: 2916-2923, 2012.
54. Jin M, Li J, Hu R, Xu B, Huang G, Huang W, Chen B, He J and Cao Y: Cyclin A2/cyclin-dependent kinase 1-dependent phosphorylation of Top2a is required for S phase entry during retinal development in zebrafish. J Genet Genomics 48: 63-74, 2021.
55. Thorenoor N, Faltejskova-Vychytilova P, Hombach S, Mlcochova J, Kretz M, Svoboda M and Slaby O: Long non-coding RNA ZFAS1 interacts with CDK1 and is involved in p53-dependent cell cycle control and apoptosis in colorectal cancer. Oncotarget 7: 622-637, 2016.
56. Fogal V, Hsieh JK, Royer C, Zhong S and Lu X: Cell cycle-dependent nuclear retention of p53 by E2F1 requires phosphorylation of p53 at Ser315. EMBO J 24: 2768-2782, 2005.
57. Aida S, Hozumi M, Ichikawa D, Iida K, Yonemura Y, Tabata N, Yamada T, Matsushita M, Sugai T, Yanagawa H and Hattori Y: A novel phenylphthalimide derivative, pegylated TC11, improves pharmacokinetic properties and induces apoptosis of high-risk myeloma cells via G2/M cell-cycle arrest. Biochem Biophys Res Commun 493: 514-520, 2017.
58. Ichikawa D, Nakamura M, Murota W, Osawa S, Matsushita M, Yanagawa H and Hattori Y: A phenylphthalimide derivative, TC11, induces apoptosis by degrading MCL1 in multiple myeloma cells. Biochem Biophys Res Commun 521: 252-258, 2020.
59. Shiheido H, Terada F, Tabata N, Hayakawa I, Matsumura N, Takashima H, Ogawa Y, Du W, Yamada T, Shoji M, *et al*: A phthalimide derivative that inhibits centrosomal clustering is effective on multiple myeloma. PLoS One 7: e38878, 2012.
60. Reid M, Agbassi YJP, Arinaminpathy N, Bercasio A, Bhargava A, Bhargava M, Bloom A, Cattamanchi A, Chaisson R, Chin D, *et al*: Scientific advances and the end of tuberculosis: A report from the lancet commission on tuberculosis. Lancet 402: 1473-1498, 2023.
61. Chandra P, Grigsby SJ and Philips JA: Immune evasion and provocation by *Mycobacterium tuberculosis*. Nat Rev Microbiol 20: 750-766, 2022.
62. Jin C, Wu X, Dong C, Li F, Fan L, Xiong S and Dong Y: EspR promotes mycobacteria survival in macrophages by inhibiting MyD88 mediated inflammation and apoptosis. Tuberculosis (Edinb) 116: 22-31, 2019.
63. Li F, Feng L, Jin C, Wu X, Fan L, Xiong S and Dong Y: LpqT improves mycobacteria survival in macrophages by inhibiting TLR2 mediated inflammatory cytokine expression and cell apoptosis. Tuberculosis (Edinb) 111: 57-66, 2018.
64. Feng L, Hu J, Zhang W, Dong Y, Xiong S and Dong C: RELL1 inhibits autophagy pathway and regulates *Mycobacterium tuberculosis* survival in macrophages. Tuberculosis (Edinb) 120: 101900, 2020.
65. Dai X, Zhou L, He X, Hua J, Chen L and Lu Y: Identification of apoptosis-related gene signatures as potential biomarkers for differentiating active from latent tuberculosis via bioinformatics analysis. Front Cell Infect Microbiol 14: 1285493, 2024.
66. Lim S and Kaldis P: Cdks, cyclins and CKIs: Roles beyond cell cycle regulation. Development 140: 3079-3093, 2013.
67. Satyanarayana A and Kaldis P: Mammalian cell-cycle regulation: Several Cdks, numerous cyclins and diverse compensatory mechanisms. Oncogene 28: 2925-2939, 2009.
68. Barnum KJ and O'Connell MJ: Cell cycle regulation by checkpoints. Methods Mol Biol 1170: 29-40, 2014.
69. Risal S, Adhikari D and Liu K: Animal models for studying the in vivo functions of cell cycle CDKs. Methods Mol Biol 1336: 155-166, 2016.
70. Zhu Y, Li K, Zhang J, Wang L, Sheng L and Yan L: Inhibition of CDK1 reverses the resistance of 5-Fu in colorectal cancer. Cancer Manag Res 12: 11271-11283, 2020.
71. Huang Z, Shen G and Gao J: CDK1 promotes the stemness of lung cancer cells through interacting with Sox2. Clin Transl Oncol 23: 1743-1751, 2021.
72. Dai Y, Hu S, Bai S, Li J, Yang N, Zhai P, Zhao B, Chen Y and Wu X: CDK1 promotes the proliferation of melanocytes in Rex rabbits. Genes Genomics 44: 1191-1199, 2022.
73. Chen Q, Xu L, Lu C, Xue Y, Gong X, Shi Y, Wang C and Yu L: Prognostic significance of CDK1 expression in diffuse large B-Cell lymphoma. BMC Cancer 25: 20, 2025.
74. Piao J, Zhu L, Sun J, Li N, Dong B, Yang Y and Chen L: High expression of CDK1 and BUB1 predicts poor prognosis of pancreatic ductal adenocarcinoma. Gene 701: 15-22, 2019.

75. Malumbres M: Cyclin-dependent kinases. Genome Biol 15: 122, 2014.
76. Kang X, Chen H, Zhou Z, Tu S, Cui B, Li Y, Dong S, Zhang Q and Xu Y: Targeting cyclin-dependent kinase 1 induces apoptosis and cell cycle arrest of activated hepatic stellate cells. Adv Biol (Weinh) 8: e2300403, 2024.
77. Hager KM and Gu W: Understanding the non-canonical pathways involved in p53-mediated tumor suppression. Carcinogenesis 35: 740-746, 2014.
78. Kang R, Kroemer G and Tang D: The tumor suppressor protein p53 and the ferroptosis network. Free Radic Biol Med 133: 162-168, 2019.
79. Kruiswijk F, Labuschagne CF and Vousden KH: p53 in survival, death and metabolic health: A lifeguard with a licence to kill. Nat Rev Mol Cell Biol 16: 393-405, 2015.
80. Bao J, He Y, Yang C, Lu N, Li A, Gao S, Hosyanto FF, Tang J, Si J, Tang X, *et al*: Inhibition of mycobacteria proliferation in macrophages by low cisplatin concentration through phosphorylated p53-related apoptosis pathway. PLoS One 18: e0281170, 2023.
81. Yuan Y, Zhang X, Du K, Zhu X, Chang S, Chen Y, Xu Y, Sun J, Luo X, Deng S, *et al*: Circ_CEA promotes the interaction between the p53 and cyclin-dependent kinases 1 as a scaffold to inhibit the apoptosis of gastric cancer. Cell Death Dis 13: 827, 2022.
82. Klingler K, Tchou-Wong KM, Brändli O, Aston C, Kim R, Chi C and Rom WN: Effects of mycobacteria on regulation of apoptosis in mononuclear phagocytes. Infect Immun 65: 5272-5278, 1997.
83. Danelishvili L, McGarvey J, Li YJ and Bermudez LE: *Mycobacterium tuberculosis* infection causes different levels of apoptosis and necrosis in human macrophages and alveolar epithelial cells. Cell Microbiol 5: 649-660, 2003.
84. Ciaramella A, Cavone A, Santucci MB, Garg SK, Sanarico N, Bocchino M, Galati D, Martino A, Auricchio G, D'Orazio M, *et al*: Induction of apoptosis and release of interleukin-1 beta by cell wall-associated 19-kDa lipoprotein during the course of mycobacterial infection. J Infect Dis 190: 1167-1176, 2004.
85. Arcila ML, Sánchez MD, Ortiz B, Barrera LF, García LF and Rojas M: Activation of apoptosis, but not necrosis, during *Mycobacterium tuberculosis* infection correlated with decreased bacterial growth: Role of TNF-alpha, IL-10, caspases and phospholipase A2. Cell Immunol 249: 80-93, 2007.
86. Lee KI, Choi S, Choi HG, Kebede SG, Dang TB, Back YW, Park HS and Kim HJ: Recombinant Rv3261 protein of *Mycobacterium tuberculosis* induces apoptosis through a mitochondrion-dependent pathway in macrophages and inhibits intracellular bacterial growth. Cell Immunol 354: 104145, 2020.
87. Medha, Priyanka, Bhatt P, Sharma S and Sharma M: Role of C-terminal domain of *Mycobacterium tuberculosis* PE6 (Rv0335c) protein in host mitochondrial stress and macrophage apoptosis. Apoptosis 28: 136-165, 2023.
88. Zychlinsky A: Programmed cell death in infectious diseases. Trends Microbiol 1: 114-117, 1993.
89. Stenger S, Mazzaccaro RJ, Uyemura K, Cho S, Barnes PF, Rosat JP, Sette A, Brenner MB, Porcelli SA, Bloom BR and Modlin RL: Differential effects of cytolytic T cell subsets on intracellular infection. Science 276: 1684-1687, 1997.
90. Kelly DM, ten Bokum AM, O'Leary SM, O'Sullivan MP and Keane J: Bystander macrophage apoptosis after *Mycobacterium tuberculosis* H37Ra infection. Infect Immun 76: 351-360, 2008.
91. Lee J, Remold HG, Ieong MH and Kornfeld H: Macrophage apoptosis in response to high intracellular burden of *Mycobacterium tuberculosis* is mediated by a novel caspase-independent pathway. J Immunol 176: 4267-4274, 2006.
92. Gan H, Lee J, Ren F, Chen M, Kornfeld H and Remold HG: *Mycobacterium tuberculosis* blocks crosslinking of annexin-1 and apoptotic envelope formation on infected macrophages to maintain virulence. Nat Immunol 9: 1189-1197, 2008.
93. Chen M, Gan H and Remold HG: A mechanism of virulence: Virulent *Mycobacterium tuberculosis* strain H37Rv, but not attenuated H37Ra, causes significant mitochondrial inner membrane disruption in macrophages leading to necrosis. J Immunol 176: 3707-3716, 2006.
94. Afriyie-Asante A, Dabla A, Dagenais A, Berton S, Smyth R and Sun J: *Mycobacterium tuberculosis* exploits focal adhesion kinase to induce necrotic cell death and inhibit reactive oxygen species production. Front Immunol 12: 742370, 2021.
95. Mohareer K, Medikonda J, Vadankula GR and Banerjee S: Mycobacterial control of host mitochondria: Bioenergetic and metabolic changes shaping cell fate and infection outcome. Front Cell Infect Microbiol 10: 457, 2020.
96. Behar SM, Martin CJ, Booty MG, Nishimura T, Zhao X, Gan HX, Divangahi M and Remold HG: Apoptosis is an innate defense function of macrophages against *Mycobacterium tuberculosis*. Mucosal Immunol 4: 279-287, 2011.
97. Dallenga T, Repnik U, Corleis B, Eich J, Reimer R, Griffiths GW and Schaible UE: M. tuberculosis-induced necrosis of infected neutrophils promotes bacterial growth following phagocytosis by macrophages. Cell Host Microbe 22: 519-530.e3, 2017.
98. Toossi Z: The inflammatory response in *Mycobacterium tuberculosis* infection. Arch Immunol Ther Exp (Warsz) 48: 513-519, 2000.
99. Amaral EP, Costa DL, Namasivayam S, Riteau N, Kamenyeva O, Mittereder L, Mayer-Barber KD, Andrade BB and Sher A: A major role for ferroptosis in *Mycobacterium tuberculosis*-induced cell death and tissue necrosis. J Exp Med 216: 556-570, 2019.
100. Su H, Zhu S, Zhu L, Huang W, Wang H, Zhang Z and Xu Y: Recombinant lipoprotein Rv1016c derived from *Mycobacterium tuberculosis* is a TLR-2 ligand that induces macrophages apoptosis and inhibits MHC II antigen processing. Front Cell Infect Microbiol 6: 147, 2016.
101. Schaible UE, Winau F, Sieling PA, Fischer K, Collins HL, Hagens K, Modlin RL, Brinkmann V and Kaufmann SH: Apoptosis facilitates antigen presentation to T lymphocytes through MHC-I and CD1 in tuberculosis. Nat Med 9: 1039-1046, 2003.
102. Velmurugan K, Chen B, Miller JL, Azogue S, Gurses S, Hsu T, Glickman M, Jacobs WR Jr, Porcelli SA and Briken V: *Mycobacterium tuberculosis* nuoG is a virulence gene that inhibits apoptosis of infected host cells. PLoS Pathog 3: e110, 2007.
103. Nisa A, Kipper FC, Panigrahy D, Tiwari S, Kupz A and Subbian S: Different modalities of host cell death and their impact on *Mycobacterium tuberculosis* infection. Am J Physiol Cell Physiol 323: C1444-C1474, 2022.
104. Kornfeld H, Mancino G and Colizzi V: The role of macrophage cell death in tuberculosis. Cell Death Differ 6: 71-78, 1999.
105. Lammas DA, Stober C, Harvey CJ, Kendrick N, Panchalingam S and Kumararatne DS: ATP-induced killing of mycobacteria by human macrophages is mediated by purinergic P2Z(P2X7) receptors. Immunity 7: 433-444, 1997.
106. Kusner DJ and Adams J: ATP-induced killing of virulent *Mycobacterium tuberculosis* within human macrophages requires phospholipase D. J Immunol 164: 379-388, 2000.
107. Laochumroonvorapong P, Paul S, Elkon KB and Kaplan G: H2O2 induces monocyte apoptosis and reduces viability of Mycobacterium avium-M. intracellulare within cultured human monocytes. Infect Immun 64: 452-459, 1996.
108. Fratazzi C, Arbeit RD, Carini C and Remold HG: Programmed cell death of Mycobacterium avium serovar 4-infected human macrophages prevents the mycobacteria from spreading and induces mycobacterial growth inhibition by freshly added, uninfected macrophages. J Immunol 158: 4320-4327, 1997.
109. Aliprantis AO, Yang RB, Mark MR, Suggett S, Devaux B, Radolf JD, Klimpel GR, Godowski P and Zychlinsky A: Cell activation and apoptosis by bacterial lipoproteins through toll-like receptor-2. Science 285: 736-739, 1999.
110. Brightbill HD, Libraty DH, Krutzik SR, Yang RB, Belisle JT, Bleharski JR, Maitland M, Norgard MV, Plevy SE, Smale ST, *et al*: Host defense mechanisms triggered by microbial lipoproteins through toll-like receptors. Science 285: 732-736, 1999.
111. Ren Y and Savill J: Apoptosis: The importance of being eaten. Cell Death Differ 5: 563-568, 1998.
112. Martin CJ, Peters KN and Behar SM: Macrophages clean up: Efferocytosis and microbial control. Curr Opin Microbiol 17: 17-23, 2014.
113. Idh J, Mekonnen M, Abate E, Wedajo W, Werngren J, Ängeby K, Lerm M, Elias D, Sundqvist T, Aseffa A, *et al*: Resistance to first-line anti-TB drugs is associated with reduced nitric oxide susceptibility in *Mycobacterium tuberculosis*. PLoS One 7: e39891, 2012.
114. Flesch IE and Kaufmann SH: Mechanisms involved in mycobacterial growth inhibition by gamma interferon-activated bone marrow macrophages: Role of reactive nitrogen intermediates. Infect Immun 59: 3213-3218, 1991.
115. Korver AJ: Amputees in a hospital of the international committee of the red cross. Injury 24: 607-609, 1993.

116. MacMicking JD, North RJ, LaCourse R, Mudgett JS, Shah SK and Nathan CF: Identification of nitric oxide synthase as a protective locus against tuberculosis. Proc Natl Acad Sci USA 94: 5243-5248, 1997.
117. Denis M: Interferon-gamma-treated murine macrophages inhibit growth of tubercle bacilli via the generation of reactive nitrogen intermediates. Cell Immunol 132: 150-157, 1991.
118. Chan J, Xing Y, Magliozzo RS and Bloom BR: Killing of virulent *Mycobacterium tuberculosis* by reactive nitrogen intermediates produced by activated murine macrophages. J Exp Med 175: 1111-1122, 1992.
119. Jamaati H, Mortaz E, Pajouhi Z, Folkerts G, Movassaghi M, Moloudizargari M, Adcock IM and Garssen J: Nitric oxide in the pathogenesis and treatment of tuberculosis. Front Microbiol 8: 2008, 2017.
120. Peteroy-Kelly M, Venketaraman V and Connell ND: Effects of *Mycobacterium bovis* BCG infection on regulation of L-arginine uptake and synthesis of reactive nitrogen intermediates in J774.1 murine macrophages. Infect Immun 69: 5823-5831, 2001.
121. Arias M, Rojas M, Zabaleta J, Rodríguez JI, París SC, Barrera LF and García LF: Inhibition of virulent *Mycobacterium tuberculosis* by Bcg(r) and Bcg(s) macrophages correlates with nitric oxide production. J Infect Dis 176: 1552-1558, 1997.
122. Dlugovitzky D, Bay ML, Rateni L, Vietti L, Farroni MA and Bottasso OA: Influence of disease severity on nitrite and cytokine production by peripheral blood mononuclear cells (PBMC) from patients with pulmonary tuberculosis (TB). Clin Exp Immunol 122: 343-349, 2000.
123. Ernst WA, Thoma-Uszynski S, Teitelbaum R, Ko C, Hanson DA, Clayberger C, Krensky AM, Leippe M, Bloom BR, Ganz T and Modlin RL: Granulysin, a T cell product, kills bacteria by altering membrane permeability. J Immunol 165: 7102-7108, 2000.
124. Chan ED, Morris KR, Belisle JT, Hill P, Remigio LK, Brennan PJ and Riches DW: Induction of inducible nitric oxide synthase-NO* by lipoarabinomannan of *Mycobacterium tuberculosis* is mediated by MEK1-ERK, MKK7-JNK, and NF-kappaB signaling pathways. Infect Immun 69: 2001-2010, 2001.